



OPEN Analysis of gas bubbling dynamics via lie symmetry approach of nonlinear wave equation

Ehab M. Almetwally¹, Rasha Saleh², Samah M. Mabrouk² & Ahmed S. Rashed²✉

Bubbles formed by the introduction of gas into a liquid are a common phenomenon, known as gas bubbling in liquids. This process is widely utilized in various industries for aeration, mixing, and purification. An optimal system of Lie symmetry analysis is employed to investigate the generalized (3 + 1)-dimensional nonlinear wave equation (NLWE). Single, double, triple, and quadruple linear combinations are constructed to derive novel solutions that represent different dynamic and turbulent behaviors of the bubbles. This equation models a wide range of nonlinear phenomena occurring in liquids containing gas bubbles. The proposed methodology is used to obtain a diverse set of accurate soliton solutions to the equation. Furthermore, the resulting solutions are analyzed in terms of their physical interpretations.

Keywords Nonlinear wave equation, Lie Infinitesimals, Optimal system, Solitons

Gas bubbling in liquids is a common phenomenon that occurs when a gas is introduced into a liquid, resulting in the formation of bubbles. This process is widely employed across various industries for mixing, aeration, and purification purposes. The characteristics of the formed bubbles, such as their size and frequency, depend on several factors, including gas flow rate, liquid viscosity, and surface tension. Overall, gas bubbling in liquids plays a crucial role in many industrial processes, rendering it a subject of significant interest to researchers and engineers alike¹. Understanding the nonlinear and shock wave dynamics involved in gas bubbling is essential for optimizing these industrial applications. Detecting and analyzing these phenomena can enhance the performance of mixing and aeration systems and improve the quality control of purified liquids. By gaining a deeper understanding of gas–liquid interactions under various conditions, researchers can devise more effective strategies for controlling and optimizing these processes. In essence, the investigation of nonlinear and shock wave dynamics in gas bubbling is fundamental to the advancement of industrial fluid dynamics.

Bubbles, regarded as inhomogeneities², play a critical role in influencing the nonlinear properties of the medium. Consequently, significant efforts have been made from various perspectives to measure the distribution of bubble sizes³. These efforts involve the application of acoustic and optical techniques, often combined with extensive computational analysis. Inhomogeneities are also present in the ocean, occurring on a much larger scale than individual bubbles. Although they may not be as visually apparent, their impact on sound propagation is considerable due to the vast distances over which sound travels in the marine environment. Local variations in sound speed arise from the mixing of water masses with different temperatures and salinities. Additionally, oceanic features such as currents, tides, eddies, and internal waves further contribute to the presence of these inhomogeneities.

The (3 + 1)-dimensional nonlinear wave equation (NLWE) can be defined as⁴:

$$(u_t + a_2 u_{xxx} + a_1 uu_x + a_3 u_x) + a_4 u_{yy} + a_5 u_{zz} = 0. \quad (1)$$

This equation provides a framework for modeling the complex interactions between waves and gas bubbles in a liquid. By incorporating the nonlinear advection term, uu_x , the dispersion term, u_{xxx} , and multidimensional effects, the equation can capture a wide range of nonlinear physical processes, such as wave–bubble interactions, bubble oscillations, sonoluminescence, and cavitation. As such, it serves as a powerful tool for investigating the rich and complex dynamics of bubbly liquids across various scientific and engineering applications^{5,6}. The nonlinear wave equation (NLWE) described in Eq. (1) has been previously examined using various analytical techniques. Hirota's bilinear method⁵ was applied to determine lump soliton and its interaction solutions for

¹Department of Mathematics and Statistics, College of Science, Imam Mohammad Ibn Saud Islamic University (IMSIU), 11432 Riyadh, Saudi Arabia. ²Department of Physics and Engineering Mathematics, Faculty of Engineering, Zagazig University, Zagazig, Egypt. ✉email: ahmed.s.rashed@gmail.com

Eq. (1) revealing two distinct dynamical behaviors: general lump-periodic and multi-kink soliton solutions. The stability of this model is examined by using the modulation instability analysis⁶, then the dynamical behavior and solutions are discussed through generalized exponential rational function method. Furthermore, Lie symmetry, multiplier, and simplest equation methods were employed on Eq. (1), leading to novel symmetry reductions, group-invariant solutions, and conservation laws⁷. Multi-soliton and periodic solutions for the NLWE with variable coefficients were reported in⁸. In addition, the linear superposition principle was used to explore special N-wave, resonant multiple wave, and complex solutions for the generalized (3 + 1)-dimensional nonlinear wave equation describing gas bubbling in liquids, as presented in⁹. Generally, nonlinear wave equations in multiple dimensions have been extensively studied using a variety of analytical techniques. Sine-Cosine^{10–14}, tanh-coth^{12,15–19}, inverse scattering^{20–22}, Hirota bilinear^{23–28}, extended homogenous method^{29–35}, Exp-function^{36–39}, Elliptic function^{40–46}, Bäcklund transformation⁴⁷, Darboux Transformation^{48,49} symmetry transformations and singular manifolds methods^{50–61} have also been employed to investigate the behavior of nonlinear partial differential equations (PDEs).

Previous research on gas bubbling dynamics has primarily concentrated on the behavior of bubbles in stagnant liquids, with relatively limited attention given to the effects of gas bubbling on fluid flow and mixing. This research paper builds upon existing knowledge by investigating how gas bubbling influences the flow patterns and turbulence levels within a liquid medium. A more comprehensive understanding of these dynamics can enable engineers to optimize process parameters, thereby improving mixing and aeration efficiency in industrial applications. The present research aims to explore the complex dynamics of gas bubbling in liquids and their implications for industrial processes. By examining the nonlinear and shock wave phenomena that arise during bubble-liquid interactions, engineers can develop more effective and energy-efficient systems for mixing and aeration. Ultimately, the goal is to enhance the overall performance, reliability, and scalability of industrial processes that rely on gas-liquid interactions. To this end, the generalized (3 + 1)-dimensional nonlinear wave equation (NLWE) is analyzed for exact solutions, including single and multiple solitons, periodic, logarithmic, exponential, and polynomial wave forms. Additionally, certain solutions are expressed in terms of arbitrary functions, which can be appropriately selected to model various physical scenarios. While the NLWE has been previously studied using different analytical techniques, the current approach, based on the Lie optimal system, yields new exact solutions that have not been reported in earlier works.

The structure of the paper is as follows. In Section “Lie transformations of NLWE”, the Lie symmetry vectors of the (3 + 1)-dimensional nonlinear wave equation (NLWE) are presented. Section “Optimal system of lie vectors” is dedicated to the reduction of the NLWE using the optimal Lie symmetry vectors. Finally, the paper concludes with a summary of the main findings in Section “Discussion of the results”.

Lie transformations of NLWE

The (3 + 1)-dimensional NLWE has the following Lie infinitesimals:

$$X_1 = \left(\frac{-1}{2a_4} y \frac{d}{dt} f_1(t) - \frac{1}{2a_5} z \frac{d}{dt} f_2(t) + f_3(t) \right) \frac{\partial}{\partial x} + f_1(t) \frac{\partial}{\partial y} + f_2(t) \frac{\partial}{\partial z} + \frac{\partial}{\partial t} + \left[-\frac{1}{2a_1 a_4} y \frac{d^2}{dt^2} f_1(t) - \frac{1}{2a_1 a_5} z \frac{d^2}{dt^2} f_2(t) + \frac{1}{a_1} \frac{d}{dt} f_3(t) \right] \frac{\partial}{\partial u}. \quad (2)$$

$$X_2 = \left(\frac{-1}{2a_4} y \frac{d}{dt} f_4(t) - \frac{1}{2a_5} z \frac{d}{dt} f_5(t) + f_6(t) \right) \frac{\partial}{\partial x} + (z + f_4(t)) \frac{\partial}{\partial y} + \left(f_5(t) - \frac{a_5}{a_4} y \right) \frac{\partial}{\partial z} + \left[-\frac{1}{2a_1 a_4} y \frac{d^2}{dt^2} f_4(t) - \frac{1}{2a_1 a_5} z \frac{d^2}{dt^2} f_5(t) + \frac{1}{a_1} \frac{d}{dt} f_6(t) \right] \frac{\partial}{\partial u}. \quad (3)$$

$$X_3 = \left(\frac{x}{2} - \frac{1}{2a_4} y \frac{d}{dt} f_7(t) - \frac{1}{2a_5} z \frac{d}{dt} f_8(t) + f_9(t) \right) \frac{\partial}{\partial x} + (y + f_7(t)) \frac{\partial}{\partial y} + (f_8(t) + z) \frac{\partial}{\partial z} + \frac{3}{2} t \frac{\partial}{\partial t} + \left[-\frac{1}{2a_1 a_4} y \frac{d^2}{dt^2} f_7(t) - \frac{1}{2a_1 a_5} z \frac{d^2}{dt^2} f_8(t) + \frac{1}{a_1} \frac{d}{dt} f_9(t) - a_1 u - a_3 \right] \frac{\partial}{\partial u}. \quad (4)$$

Here, the (3 + 1)-dimensional nonlinear wave equation (NLWE) is considered, in which arbitrary functions appear within the Lie symmetry vectors. These functions are determined through an optimization process that aims to reduce the number of vectors involved in the commutator products. The commutator products of these vectors are given as follows:

$$\begin{aligned}
 [X_1, X_2] = & \left(\frac{-1}{2a_4} f_1 f_4' - \frac{1}{2a_5} f_2 f_5' + f_6' + \frac{1}{2a_4} f_4 f_1' + \frac{1}{2a_5} f_5 f_2' + y \left(\frac{-1}{2a_4} f_4'' - \frac{1}{2a_4} f_2' \right) \right. \\
 & + z \left(\frac{-1}{2a_5} f_5'' + \frac{1}{2a_4} f_1' \right) \left. \frac{\partial}{\partial x} + \left(f_2 + f_4' \right) \frac{\partial}{\partial y} + \left(\frac{-a_5}{a_4} f_1 + f_5' \right) \frac{\partial}{\partial z} \right. \\
 & + \left(\frac{-1}{2a_4 a_1} f_4' f_1 - \frac{1}{2a_5 a_1} f_5' f_2 + \frac{1}{a_1} f_6'' + \frac{1}{2a_4 a_1} f_1' f_4 + \frac{1}{2a_5 a_1} f_2' f_5 \right. \\
 & \left. + z \left(\frac{-1}{2a_5 a_1} f_5''' + \frac{1}{2a_4 a_1} f_1'' \right) + y \left(\frac{-1}{2a_4 a_1} f_4''' - \frac{1}{2a_4 a_1} f_2'' \right) \right) \frac{\partial}{\partial u}.
 \end{aligned} \tag{5}$$

$$\begin{aligned}
 [X_1, X_3] = & \left(\frac{-1}{2a_4} f_1 f_7' - \frac{1}{2a_5} f_2 f_8' + \frac{1}{2} f_3 + f_9' + \frac{1}{2a_4} f_7 f_1' + \frac{1}{2a_5} f_8 f_2' - \frac{3}{2} t f_3' \right. \\
 & + y \left(\frac{1}{4a_4} f_1' - \frac{1}{2a_4} f_7'' + \frac{3}{4a_4} t f_1'' \right) + z \left(\frac{1}{4a_5} f_2' - \frac{1}{2a_5} f_8'' + \frac{3}{4a_5} t f_2'' \right) \left. \frac{\partial}{\partial x} \right. \\
 & + \left(f_1 + f_7' - \frac{3}{2} t f_1' \right) \frac{\partial}{\partial y} + \left(f_2 + f_8' - \frac{3}{2} t f_2' \right) \frac{\partial}{\partial z} + \left(\frac{-1}{2a_4 a_1} f_7' f_1 - \frac{1}{2a_5 a_1} f_8' f_2 \right. \\
 & - \frac{3}{2a_1} t f_3'' - \frac{1}{a_1} f_3' + \frac{1}{a_1} f_9'' + \frac{1}{2a_4 a_1} f_1' f_7 + \frac{1}{2a_5 a_1} f_2' f_8 + z \left(\frac{3}{4a_5 a_1} t f_2''' + \frac{1}{a_5 a_1} f_2'' \right. \\
 & \left. - \left(\frac{3}{4a_5 a_1} t f_2''' + \frac{1}{a_5 a_1} f_2'' - \frac{1}{2a_4 a_1} f_8''' \right) + y \left(\frac{3}{4a_4 a_1} t f_1''' + \frac{1}{a_4 a_1} f_1'' - \frac{1}{2a_4 a_1} f_7''' \right) \right) \frac{\partial}{\partial u}.
 \end{aligned} \tag{6}$$

$$\begin{aligned}
 [X_2, X_3] = & \left(\frac{-1}{2a_4} f_4 f_7' - \frac{1}{2a_5} f_5 f_8' + \frac{1}{2} f_6 - \frac{3}{2} t f_6' + \frac{1}{2a_4} f_7 f_4' \right. \\
 & + \frac{1}{2a_5} f_8 f_5' + y \left(\frac{1}{4a_4} f_4' + \frac{1}{2a_4} f_8' + \frac{3}{4a_4} t f_4'' \right) + z \left(\frac{1}{4a_5} f_5' - \frac{1}{2a_5} f_7' + \frac{3}{4a_5} t f_5'' \right) \left. \frac{\partial}{\partial x} \right. \\
 & + \left(f_4 - f_8 - \frac{3}{2} t f_4' \right) \frac{\partial}{\partial y} + \left(f_5 + \frac{a_5}{a_4} f_7 - \frac{3}{2} t f_5' \right) \frac{\partial}{\partial z} \\
 & + \left(\frac{-1}{2a_4 a_1} f_7' f_4 - \frac{1}{2a_5 a_1} f_8' f_5 - \frac{3}{2a_1} t f_6'' - \frac{1}{a_1} f_6' + \frac{1}{2a_4 a_1} f_4' f_7 \right. \\
 & \left. + \frac{1}{2a_5 a_1} f_5' f_8 + z \left(\frac{3}{4a_5 a_1} t f_5''' + \frac{1}{a_5 a_1} f_5'' - \frac{1}{2a_4 a_1} f_7'' \right) + y \left(\frac{3}{4a_4 a_1} t f_4''' + \frac{1}{a_4 a_1} f_4'' + \frac{1}{2a_4 a_1} f_8'' \right) \right) \frac{\partial}{\partial u}.
 \end{aligned} \tag{7}$$

These commutative products^{51,53,62} leads to a system of ordinary differential equations (ODEs) in $f_i(t)$ in the following form:

$$\left. \begin{aligned}
& \frac{-1}{2a_4} f_1 f_4' - \frac{1}{2a_5} f_2 f_5' + f_6' + \frac{1}{2a_4} f_4 f_1' \\
& + \frac{1}{2a_5} f_5 f_2' = 0, \quad \frac{-1}{2a_4} f_4'' - \frac{1}{2a_4} f_2' = 0, \\
& \frac{-1}{2a_5} f_5'' + \frac{1}{2a_4} f_1' = 0, \\
& f_2 + f_4' = 0, \quad \frac{-a_5}{a_4} f_1 + f_5' = 0, \\
& \frac{-1}{2a_5 a_1} f_5''' + \frac{1}{2a_4 a_1} f_1'' = 0, \\
& \frac{-1}{2a_4 a_1} f_4'' f_1 - \frac{1}{2a_5 a_1} f_5'' f_2 + \frac{1}{a_1} f_6'' + \frac{1}{2a_4 a_1} f_1'' f_4 + \frac{1}{2a_5 a_1} f_2'' f_5 = 0, \\
& \frac{-1}{2a_4 a_1} f_4''' - \frac{1}{2a_4 a_1} f_2'' = 0, \\
& \frac{-1}{2a_4} f_1 f_7' - \frac{1}{2a_5} f_2 f_8' - f_3 + f_9' + \frac{1}{2a_4} f_7 f_1' + \frac{1}{2a_5} f_8 f_2' - \frac{3}{2} t f_3' = 0, \\
& \frac{1}{a_4} f_1' - \frac{1}{2a_4} f_7'' + \frac{3}{4a_4} t f_1'' = 0, \\
& \frac{1}{a_5} f_2' - \frac{1}{2a_5} f_8'' + \frac{3}{4a_5} t f_2'' = 0, \\
& 2f_7' - f_1 - 3t f_1' = 0, \\
& 2f_8' - f_2 - 3t f_2' = 0, \\
& \frac{-1}{2a_4 a_1} f_7'' f_1 - \frac{1}{2a_5 a_1} f_8'' f_2 - \frac{3}{2a_1} t f_3'' - \frac{5}{2a_1} f_3' \\
& + \frac{1}{a_1} f_9'' + \frac{1}{2a_4 a_1} f_1'' f_7 + \frac{1}{2a_5 a_1} f_2'' f_8 = 0, \\
& \frac{3}{4a_5 a_1} t f_2''' + \frac{7}{4a_5 a_1} f_2'' - \frac{1}{2a_4 a_1} f_8''' = 0, \\
& \frac{3}{4a_4 a_1} t f_1''' + \frac{7}{4a_4 a_1} f_1'' - \frac{1}{2a_4 a_1} f_7''' = 0, \\
& \frac{-1}{2a_4} f_4 f_7' - \frac{1}{2a_5} f_5 f_8' + \frac{1}{2} f_6 - \frac{3}{2} t f_6' + \frac{1}{2a_4} f_7 f_4' + \frac{1}{2a_5} f_8 f_5' = 0, \\
& \frac{1}{4a_4} f_4' + \frac{1}{2a_4} f_8' + \frac{3}{4a_4} t f_4'' = 0, \\
& \frac{1}{4a_5} f_5' - \frac{1}{2a_5} f_7' + \frac{3}{4a_5} t f_5'' = 0, \\
& f_4 - f_8 - \frac{3}{2} t f_4' = 0, \\
& f_5 + \frac{a_5}{a_4} f_7 - \frac{3}{2} t f_5' = 0, \\
& \frac{-1}{2a_4 a_1} f_7'' f_4 - \frac{1}{2a_5 a_1} f_8'' f_5 - \frac{3}{2a_1} t f_6'' - \frac{1}{a_1} f_6' \\
& + \frac{1}{2a_4 a_1} f_4'' f_7 + \frac{1}{2a_5 a_1} f_5'' f_8 = 0, \\
& \frac{3}{4a_5 a_1} t f_5''' + \frac{1}{a_5 a_1} f_5'' - \frac{1}{2a_4 a_1} f_7'' = 0, \\
& \frac{3}{4a_4 a_1} t f_4''' + \frac{1}{a_4 a_1} f_4'' + \frac{1}{2a_4 a_1} f_8'' = 0.
\end{aligned} \right\} \quad (8)$$

This system of differential equations has infinite number of solutions. One of the obtained results are given by the following eighteen vectors.

$$\begin{aligned}
X_1 &= \frac{\partial}{\partial y} + \frac{\partial}{\partial t}, X_2 = \frac{\partial}{\partial z} + \frac{\partial}{\partial t}, X_3 = \frac{\partial}{\partial x} + \frac{\partial}{\partial t}, X_4 = t \frac{\partial}{\partial x} + \frac{\partial}{\partial t} + \frac{\partial}{\partial u}, \\
X_5 &= \frac{\partial}{\partial x} + z \frac{\partial}{\partial y} - y \frac{\partial}{\partial z}, X_6 = t \frac{\partial}{\partial x} + z \frac{\partial}{\partial y} - y \frac{\partial}{\partial z} + \frac{\partial}{\partial u}, X_7 = z \frac{\partial}{\partial y} + (1-y) \frac{\partial}{\partial z}, \\
X_8 &= -\frac{y}{2} \frac{\partial}{\partial x} + t \frac{\partial}{\partial y} + \frac{\partial}{\partial t}, X_9 = -\frac{z}{2} \frac{\partial}{\partial x} + t \frac{\partial}{\partial z} + \frac{\partial}{\partial t}, X_{10} = (z+1) \frac{\partial}{\partial y} - y \frac{\partial}{\partial z}, \\
X_{11} &= -\frac{z}{2} \frac{\partial}{\partial x} + z \frac{\partial}{\partial y} + (t-y) \frac{\partial}{\partial z}, X_{12} = -\frac{y}{2} \frac{\partial}{\partial x} + (t+z) \frac{\partial}{\partial y} - y \frac{\partial}{\partial z},
\end{aligned}$$

$$\begin{aligned}
X_{13} &= \left(t + \frac{x}{2}\right) \frac{\partial}{\partial x} + y \frac{\partial}{\partial y} + z \frac{\partial}{\partial z} + \frac{3t}{2} \frac{\partial}{\partial t} - u \frac{\partial}{\partial u}, \\
X_{14} &= \left(1 + \frac{x}{2}\right) \frac{\partial}{\partial x} + y \frac{\partial}{\partial y} + z \frac{\partial}{\partial z} + \frac{3t}{2} \frac{\partial}{\partial t} - (u+1) \frac{\partial}{\partial u}, \\
X_{15} &= \left(\frac{x}{2}\right) \frac{\partial}{\partial x} + (y+1) \frac{\partial}{\partial y} + z \frac{\partial}{\partial z} + \frac{3t}{2} \frac{\partial}{\partial t} - (u+1) \frac{\partial}{\partial u}, \\
X_{16} &= \left(\frac{x}{2}\right) \frac{\partial}{\partial x} + y \frac{\partial}{\partial y} + (z+1) \frac{\partial}{\partial z} + \frac{3t}{2} \frac{\partial}{\partial t} - (u+1) \frac{\partial}{\partial u}, \\
X_{17} &= \left(\frac{x-y}{2}\right) \frac{\partial}{\partial x} + (y+t) \frac{\partial}{\partial y} + z \frac{\partial}{\partial z} + \frac{3t}{2} \frac{\partial}{\partial t} - (u+1) \frac{\partial}{\partial u}, \\
X_{18} &= \left(\frac{x-z}{2}\right) \frac{\partial}{\partial x} + y \frac{\partial}{\partial y} + (z+t) \frac{\partial}{\partial z} + \frac{3t}{2} \frac{\partial}{\partial t} - (u+1) \frac{\partial}{\partial u}.
\end{aligned} \tag{9}$$

Optimal system of lie vectors

Lie vectors are mathematically defined as the infinitesimal generators of a Lie group, enabling the precise characterization of small transformations within the group. They play a fundamental role in the study of Lie groups and their applications across various fields, including differential geometry, physics, and robotics. An appropriate selection of Lie vectors is essential for accurately describing group transformations and for simplifying computations in these areas. By carefully selecting suitable Lie vectors, one can significantly improve both the computational efficiency and the accuracy of algorithms that rely on Lie theory. To this end, systematic procedures based on the concepts of commutation relations, Eq. (10), and the adjoint representation, Eq. (11), are employed to identify the optimal system of vectors, including single, double, triple, and quadruple linear combinations.

$$[X_i, X_j] = X_i X_j - X_j X_i. \tag{10}$$

$$Ad(exp(\varepsilon v))w_0 = \sum_{n=0}^{\infty} \frac{\varepsilon^n}{n!} (adv)^n(w_0) = w_0 - \varepsilon[v, w_0] + \frac{\varepsilon^2}{2}[v, [v, w_0]] - \dots \tag{11}$$

To avoid much mathematical analysis, more details about commutator tables, adjoint matrix, and optimal system representation can be found in^{51,53}.

Reduction using single vectors

The optimization procedure leads to the following optimal single vectors: $X_6, X_7, X_9, X_{10}, X_{12}, X_{13}, X_{16}$ and X_{18} . Moreover, the dual combinations were found to be $X_6 + X_{10}, X_7 + X_{10}, X_{10} + X_{12}, X_7 + X_{16}, X_9 + X_{16}, X_{13} + X_{16}, X_{13} + X_{18}$, the triple combinations were defined as $X_6 + X_7 + X_{10}, X_6 + X_7 + X_{12}, X_6 + X_{10} + X_{12}, X_7 + X_{10} + X_{12}, X_9 + X_{13} + X_{18}, X_{13} + X_{16} + X_{18}$. Moreover, only one quadruple combination is obtained after considering the simplification of adjoint matrices^{51,53}. This combination is $X_{12} + X_{13} + X_{16} + X_{18}$. These vectors are used sequentially to detect exact solutions of NLWE^{63–66}.

Case 1: using X_6

This vector is used to reduce the number of independent variables of Eq. (1) and transform it to be:

$$pw_{rrrr} + (p + q^2 + pw) w_{rr} + 4p \left(pw_{pp} + \frac{1}{4} w_r^2 + w_p + \frac{1}{4} w_{rq} \right) = 0, \tag{12}$$

where, $p = y^2 + z^2, q = t, r = -\arctan\left(\frac{y}{z}\right) + x, w = u - \arctan\left(\frac{y}{z}\right)$.

Now, Eq. (12) is tested for Lie vectors using MAPLE to obtain one of its infinitesimal vectors in the form, $Y = q \frac{\partial}{\partial r} + \frac{\partial}{\partial w}$. This vector is employed to reduce the Eq. (12) into:

$$4sv_{ss} + 4v_s = 0. \tag{13}$$

Where, $o = q, s = p, v(s, o) = w(p, q, r) - \frac{r}{q}$. This equation has an exact solution in the form:

$$v(s, o) = F_1(o) + F_2(o) \ln(s). \tag{14}$$

where, F_1 and F_2 are arbitrary functions in their arguments.

Finally, the solution of Eq. (1) can be formulated in the form:

$$u_1(x, y, z, t) = \arctan\left(\frac{y}{z}\right) + F_2(t) \ln(y^2 + z^2) + F_1(t). \tag{15}$$

The behavior of the gas bubbles is depicted in Fig. 1 for $F_1(t) = e^{-t^2}, F_2(t) = \frac{\sin^2(t)}{t}$.

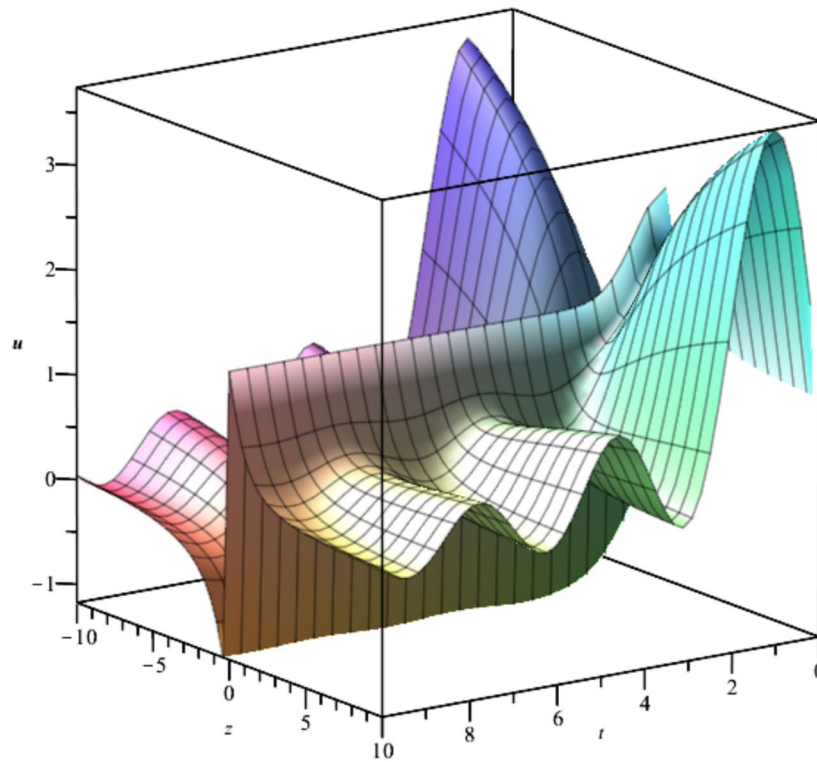


Fig. 1. Illustration of $u_1(x, y, z, t)$ for $F_1(t) = e^{-t^2}$, $F_2(t) = \frac{\sin^2(t)}{t}$, $y = 1$.

Case 2: using X_7

This vector is used to reduce the number of independent variables in Eq. (1), resulting in:

$$w_{pppp} + (1 + w)w_{pp} + (4 + 4q)w_{qq} + w_p^2 + 4w_q + w_{pr} = 0, \quad (16)$$

Where, $p = x$, $q = y^2 + z^2 - 2y$, $r = t$, $w(p, q, r) = u(x, y, z, t)$.

This equation has Lie infinitesimal vectors. One of these vectors is $(1 + \frac{p}{4})\frac{\partial}{\partial p} + (q + 1)\frac{\partial}{\partial q} + (\frac{3r}{4})\frac{\partial}{\partial r} - (\frac{w+1}{2})\frac{\partial}{\partial w}$.

The invariant transformation is defined by:

$$o = \frac{r}{(p+4)^3}, s = \frac{q+1}{p^4 + 16p^3 + 96p^2 + 256p + 256},$$

$$v(s, o) = p^2w(p, q, r) + p^2 + 8pw(p, q, r) + 8p + 16w(p, q, r). \quad (17)$$

This transformation transforms Eq. (16) into:

$$\begin{aligned} & o^4v_{oooo} + \frac{16}{3}o^3sv_{ooos} + \frac{32}{3}o^2s^2v_{ooss} + \frac{256}{27}os^3v_{oss} + \frac{256}{81}s^4v_{ssss} + \frac{32}{3}o^3v_{ooo} \\ & + \frac{136}{3}o^2sv_{oos} + 64os^2v_{oss} + \frac{2432}{81}s^3v_{sss} + \frac{o}{9}\left(ov + 276o - \frac{1}{3}\right)v_{oo} \\ & + \frac{8s}{27}\left(ov + 320o - \frac{1}{6}\right)v_{os} + \frac{16s}{81}\left(sv + 367s + \frac{1}{4}\right)v_{ss} + \frac{o^2}{9}v_o^2 + \left(-\frac{5}{81} + \frac{4}{9}ov + \frac{8os}{27}v_s + \frac{712o}{27}\right)v_o \\ & + \frac{16s^2}{81}v_s^2 + \left(\frac{4}{81} + \frac{52s}{81}v + \frac{3736s}{81}\right)v_s + \frac{10}{81}(28 + v)(16 + v) = 0. \end{aligned} \quad (18)$$

Equation (18) has a Lie vector in the form; $(so^{\frac{1}{3}})\frac{\partial}{\partial s} + \left(\frac{3}{4}o^{\frac{4}{3}}\right)\frac{\partial}{\partial o} - \left(\frac{1+o(6v+96)}{12o^{\frac{2}{3}}}\right)\frac{\partial}{\partial v}$ which transforms the equation to:

$$81\alpha^4\phi_{\alpha\alpha} + 189\alpha^3\phi_{\alpha} + 36\alpha^2\phi - 8 = 0, \quad (19)$$

where, $\alpha = os^{-\frac{3}{4}}$, $\phi(\alpha) = \sqrt{s}\left(-\frac{1}{3o} + v(s, o) + 16\right)$.

Now, Eq. (19) could be solved analytically. Using Back substitutions, the solution of Eq. (1) is formulated in the form:

$$u_2(x, y, z, t) = \frac{1}{36t^{\frac{8}{3}}} \left(36C_1 t^2 \ln(t) - 27C_1 t^2 \ln(y^2 + z^2 - 2y + 1) \right) - 36t^{\frac{8}{3}} + 12xt^{\frac{5}{3}} + 2y^2 t^{\frac{2}{3}} + 2z^2 t^{\frac{2}{3}} + 36C_2 t^2 + 48t^{\frac{5}{3}} - 4yt^{\frac{2}{3}} + 2t^{\frac{2}{3}}. \quad (20)$$

The bubble dynamics is illustrated in Fig. 2

Case 3: using X_9

Similar procedures are being used to extract and create new families of solutions for NLWE in its three-dimensional form. The vector X_9 transforms Eq. (1) into:

$$w_{rrrr} + \left(1 + w - \frac{q}{4} \right) w_{rr} + w_r^2 + w_{pp} + 4w_{qq} = 0, \quad (21)$$

where, $p = y, q = t^2 - 2z, r = \frac{1}{6}(3tz - t^3) + x, w(p, q, r) = u(x, y, z, t)$.

At this stage, Eq. (21) undergoes the Lie infinitesimal test, which yields a number of infinitesimal generators. These generators, along with their associated reduction procedures, are summarized in Table 1.

The solutions, u_3, u_4 and u_5 are illustrated in Figs. 3, 4 and 5.

Case 4: using X_{10}

This vector transforms Eq. (1) to:

$$w_p^2 + ww_{pp} - 2qw_{qq} + w_{pr} + w_{ppp} + w_{pp} + w_{qq} - 2w_q = 0, \quad (22)$$

where, $p = x, q = -\left(\frac{z^2 + y^2}{2}\right) - z, r = t, w = u$.

Equation (22) has an infinitesimal vector, $\left(\frac{p}{2} + 1\right) \frac{\partial}{\partial p} + (2q - 1) \frac{\partial}{\partial q} + \frac{3r}{2} \frac{\partial}{\partial r} - (w + 1) \frac{\partial}{\partial w}$.

Following the same procedures, the following solution can be obtained.

$$u_6 = \frac{1}{36t^{\frac{14}{3}}} \left(-27C_1 t^4 \ln(-y^2 - z^2 - 2z - 1) + t^{\frac{8}{3}} (2y^2 + 2z^2 + 4z + 2) \right. \\ \left. + 27C_1 \ln(2) t^4 + 36C_1 t^4 \ln(t) - 36t^{\frac{14}{3}} + 36C_2 t^4 + t^{\frac{11}{3}} (24 + 12x) \right). \quad (23)$$

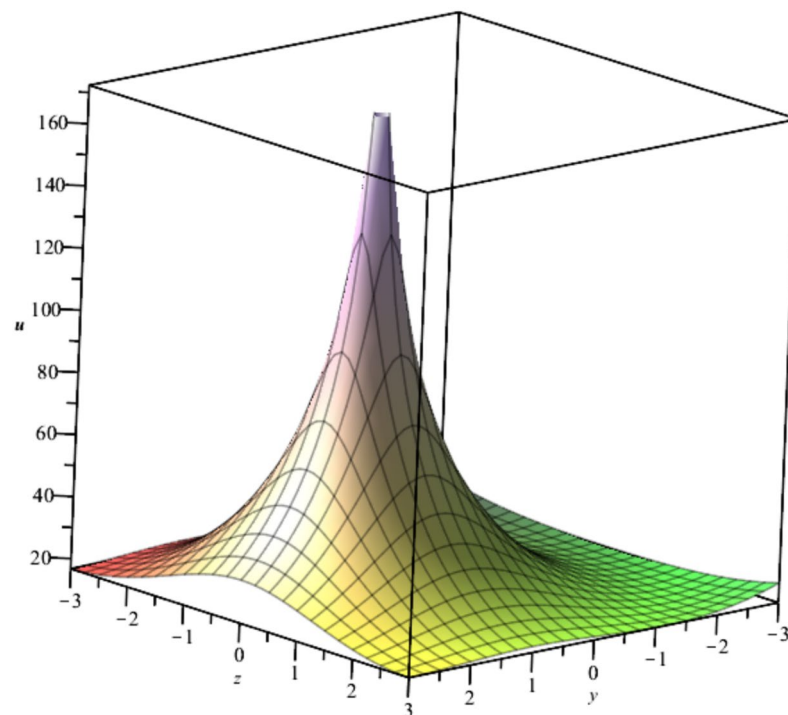


Fig. 2. Illustration of $u_2(x, y, z, t)$ at $x = 1, t = 1, C_1 = C_2 = 1$.

Case 3.1	Vector	$\frac{\partial}{\partial r}$
	Reduced Form	$v_{ss} + 4v_{oo} = 0$, Where, $o = q, s = p, v(s, o) = w(p, q, r)$.
	Solution	$v(s, o) = F_1(o - 2Is) + F_2(o + 2Is)$
	Final Solution of (1)	$u_3 = F_1(t^2 - 2z - 2Iy) + F_2(t^2 - 2z + 2Iy)$.
Case 3.2	Vector	$\frac{\partial}{\partial q} + \frac{1}{4}\frac{\partial}{\partial w}$
	Reduced Form	$v_o^2 + v_{ss} + (1 + v)v_{oo} + v_{ooo} = 0$, Where, $o = r, s = p, v(s, o) = w(p, q, r) - \frac{q}{4}$.
	Solution	$v(s, o) = -12C_3^2 \tanh^2(C_2s + C_3o + C_1) - \frac{C_2^2 + C_3^2 - 8C_3^4}{C_3^2}$
	Final Solution of (1)	$u_4 = t^2 - \frac{z}{2} - 12C_3^2 \tanh^2\left(C_1 + C_2y + C_3\left(x + \frac{3tz - t^3}{6}\right)\right) - \frac{C_2^2 + C_3^2 - 8C_3^4}{C_3^2}$.
Case 3.3	Vector	$q\frac{\partial}{\partial p} - 4p\frac{\partial}{\partial q} - p\frac{\partial}{\partial w}$.
	Reduced Form 1	$vv_{oo} + v_o^2 + 16sv_{ss} + v_{ooo} + v_{oo} + 16v_s = 0$, Where, $o = r, s = 4p^2 + q^2, v = w - \frac{q}{4}$
	New level vector	$\frac{\partial}{\partial o}$
	Reduced Form 2	$\alpha\phi_{\alpha\alpha} + \phi_{\alpha} = 0$, Where, $\alpha = s, \phi = v$
	Solution	$\phi = C_1 + C_2 \ln(\alpha)$.
	Final Solution of (1)	$u_5 = C_1 + \frac{t^2}{4} - \frac{z}{2} + C_2 \ln\left(4y^2 + (t^2 - 2z)^2\right)$.

Table 1. Lie Infinitesimal Vectors of Eq. (21) Using X_9 .

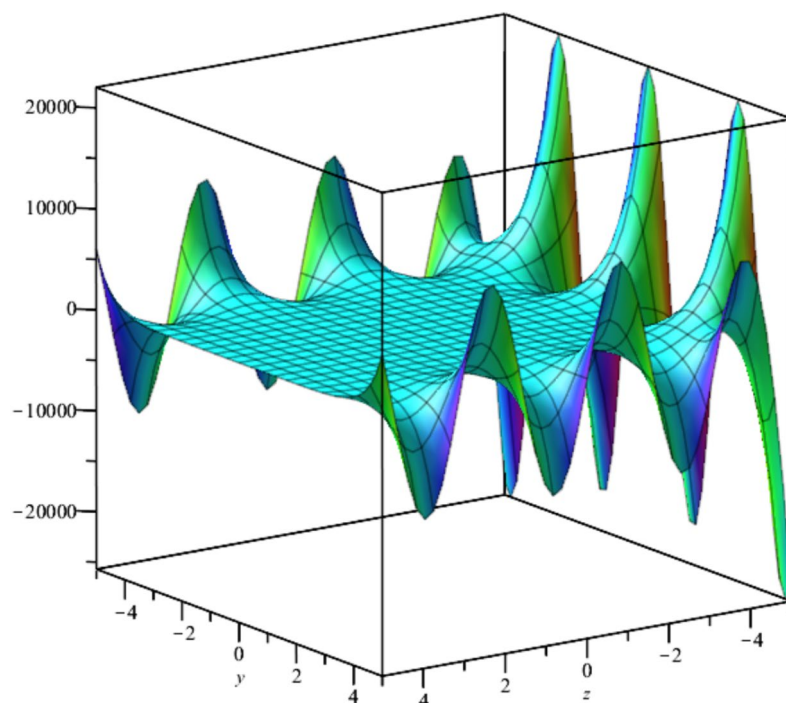


Fig. 3. Illustration of u_3 at $t = 0$ For $F_1 = \exp(t^2 - 2z - 2Iy)$, $F_2 = \sin(t^2 - 2z + 2Iy)$.

The behavior of the solution described by (23) is depicted hereafter in Fig. 6.

Case 5: using X_{12}

Using the invariant variables, $P = z - 2x, q = t, r = 4x(z - 2x) + 4tx + 4x^2 + y^2, w(p, q, r) = u(x, y, z, t)$. the following solution is obtained.

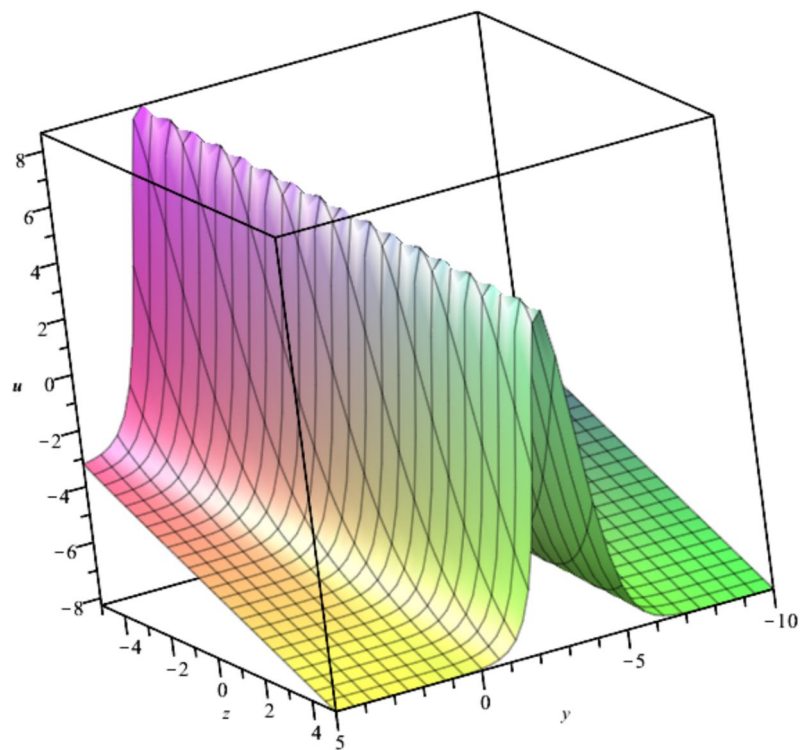


Fig. 4. Illustration of u_4 at $C_1 = C_2 = C_3 = 1, x = 0, t = 1$.

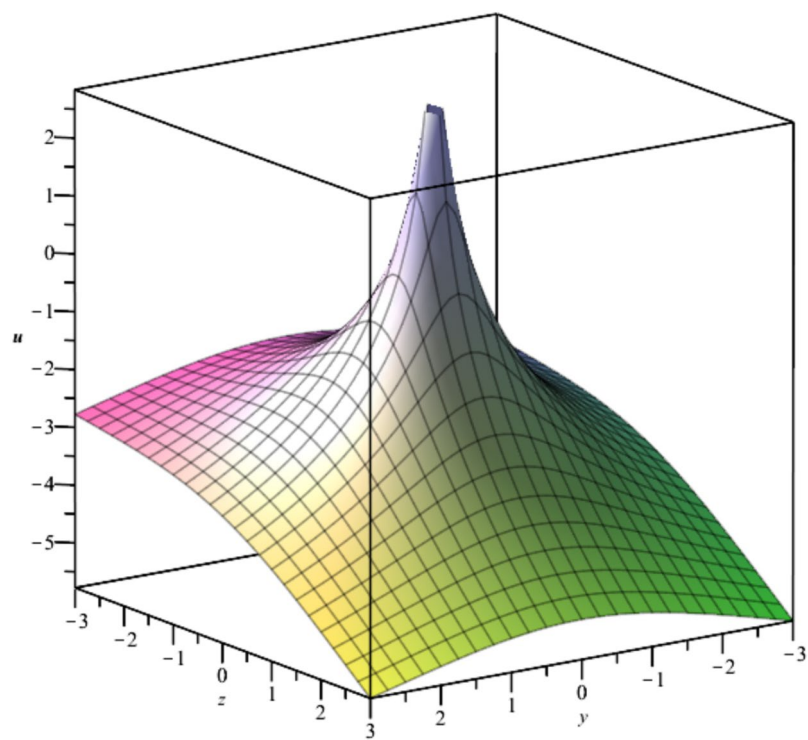


Fig. 5. Illustration of u_5 at $C_1 = 0, C_2 = -1, t = 0$.

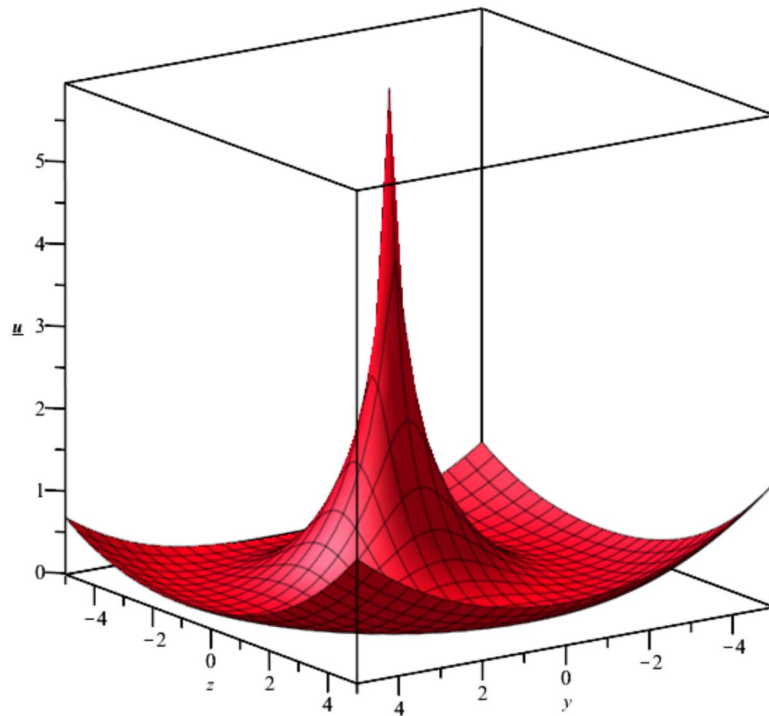


Fig. 6. Illustration of u_6 at $C_1 = C_2 = 1, x = 0, t = 1$.

$$u_7 = C_1 - \frac{t}{2} + C_2 \ln(t^2 + 2tz + y^2 + z^2). \quad (24)$$

The behavior of the gas bubble due to the case in Eq. (24) is illustrated in Fig. 7

Case 6: using X_{13}

The invariant variables of X_{13} are $p = \frac{z}{y}, q = ty^{-\frac{3}{2}}, r = \frac{x-t}{\sqrt{y}}, w = yu$. The transformed equation is given by:

$$\begin{aligned} &6rqw_{qr} + r^2w_{rr} + 9q^2w_{qq} + 12pqw_{pq} + 4rpw_{pr} \\ &+ 4p^2w_{pp} + 4w_r^2 + 7rw_r + 4ww_{rr} + 27qw_q \\ &+ 16pw_p + 4w_{qr} + 4w_{rrrr} + 8w + 4w_{pp} = 0. \end{aligned} \quad (25)$$

The new equation admits three infinitesimal Lie generators. The following subcases are derived and presented in Table 2. The solution, u_8 , is depicted in Fig. 8.

Case 7: using X_{16}

This vector results in three distinct solutions that are given in the following forms:

$$u_{11} = C_1 t^{-\frac{2}{3}} \ln(t) - \frac{3}{4} C_1 t^{-\frac{2}{3}} \ln(y^2 + z^2 + 2z + 1) + \frac{x}{3t} + \frac{y^2 + z^2}{18t^2} + C_2 t^{-\frac{2}{3}} + \frac{2z + 1}{18t^2} - 1. \quad (26)$$

$$u_{12} = \frac{(-y^2 + y(C_1 - \frac{C_0}{2}) - (z + 1)(z + 1 - C_2))}{(y^2 + (z + 1)^2)} + t^{-\frac{7}{3}} \left(C_2 ty + \frac{1}{9} t^{\frac{1}{3}} y^2 + \frac{x}{3} t^{\frac{4}{3}} + C_1 t^{\frac{5}{3}} \right). \quad (27)$$

$$u_{13} = \frac{x}{3t} + C_2 t^{-\frac{2}{3}} + \frac{y^2}{9t^2} + C_1 t^{-\frac{4}{3}} (z + 1) - 1. \quad (28)$$

Case 8: using X_{18}

Another three exact solutions can be obtained as follows:

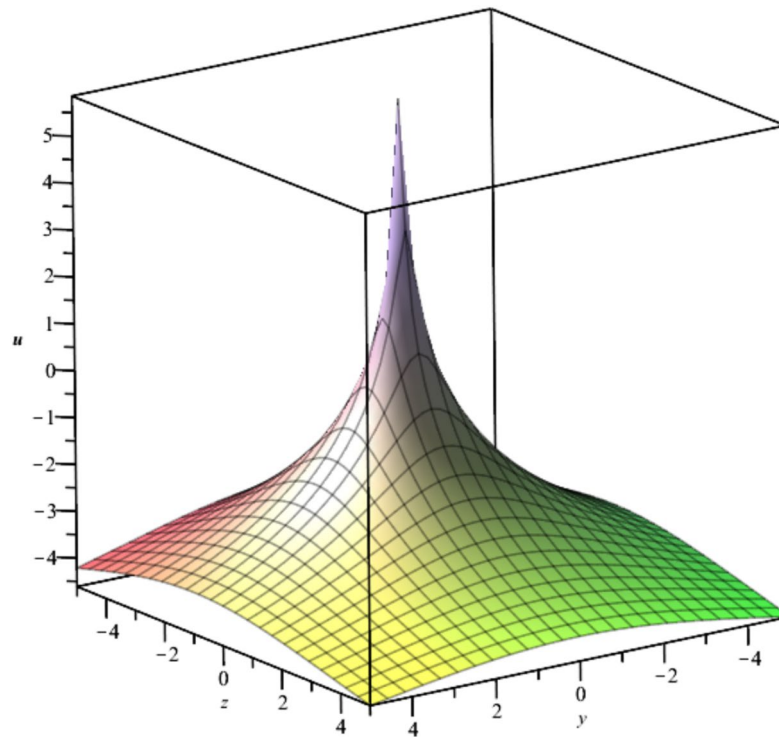


Fig. 7. Illustration of u_7 at $C_1 = 0, C_2 = -1, t = 1$.

Case 6.1	Vector	$q^{\frac{1}{3}} \frac{\partial}{\partial r} + \frac{1}{3} q^{-\frac{2}{3}} \frac{\partial}{\partial w}.$
	Reduced Form	$36o^2 (s^2 + 1) v_{ss} + 81o^4 v_{oo} + 108so^3 v_{os} + 243o^3 v_o + 144so^2 v_s + 72o^2 v - = 0.$
	Solution	$v(s, o) = \frac{C_0 s^2 + 2C_2 s + 2C_1}{2(s^2 + 1)} + \frac{2-9C_0 o^2}{18o^2} + C_1 o^{-\frac{2}{3}} + C_2 o^{-\frac{4}{3}}.$
	Final Solution of (1)	$u_8 = \frac{1}{t^{\frac{7}{3}} (y^2 + z^2)} \left(t^{\frac{7}{3}} \left(-\frac{y^2}{3} + y \left(C_1 - \frac{C_0}{2} \right) - \frac{z(z-3C_2)}{3} \right) + (y^2 + z^2) \left(C_2 t y + \frac{1}{9} t^{\frac{1}{3}} y^2 + \frac{1}{3} x t^{\frac{4}{3}} + C_1 t^{\frac{5}{3}} \right) \right).$
Case 6.2	Vector	$q^{\frac{2}{3}} \frac{\partial}{\partial p} - \left(\frac{p}{3q^{\frac{1}{3}}} \right) \frac{\partial}{\partial r} + \left(\frac{p}{9q^{\frac{4}{3}}} \right) \frac{\partial}{\partial w}.$
	Reduced Form 1	$36s^2 v_{oooo} + 9s^2 (o^2 + 4v) v_{oo} + (54os^3 + 36s^2) v_{os} + 81s^4 v_{ss} + 36s^2 v_o^2 + (63os^2 + 12s) v_o + 243s^3 v_s + 72s^2 v + 4 = 0.$
	New level vector	$s^{\frac{1}{3}} \frac{\partial}{\partial o} + \frac{1}{3} s^{-\frac{2}{3}} \frac{\partial}{\partial v}.$
	Reduced Form 2	$9\alpha^2 \phi_{\alpha\alpha} + 27\alpha \phi_{\alpha} + 8\phi = 0$
	Solution	$\phi(\alpha) = C_1 \alpha^{-\frac{2}{3}} + C_2 \alpha^{-\frac{4}{3}}.$
	Final Solution of (1)	$u_9 = 9C_1 t^{-\frac{2}{3}} + 9C_2 y t^{-\frac{4}{3}} - \frac{1}{3} + \frac{x}{3t} + \frac{1}{9} t^{-2} z^2.$
Case 6.3	Vector	$\left(p^2 + 1 \right) \frac{\partial}{\partial p} + \left(\frac{3pq}{2} \right) \frac{\partial}{\partial q} + \left(\frac{pr}{2} \right) \frac{\partial}{\partial r} - (pw) \frac{\partial}{\partial w}.$
	Reduced Form 1	$4v_{oooo} + (o^2 + 4v) v_{oo} + 6osv_{os} + 9s^2 v_{ss} + 5ov_o + 21sv_s + 4v_o^2 + 4v = 0.$
	New level vector	$s^{\frac{1}{3}} \frac{\partial}{\partial o} + \frac{1}{3} s^{-\frac{2}{3}} \frac{\partial}{\partial v}.$
	Reduced Form 2	$81\alpha^4 \phi_{\alpha\alpha} + 189\alpha^3 \phi_{\alpha} + 36\alpha^2 \phi - 8 = 0.$
	Solution	$\phi(\alpha) = C_1 \alpha^{-\frac{2}{3}} \ln(\alpha) + C_2 \alpha^{-\frac{2}{3}} + \frac{1}{18\alpha^2}.$
	Final Solution of (1)	$u_{10} = \frac{1}{36t^{\frac{8}{3}}} \left(-12t^{\frac{8}{3}} + 12xt^{\frac{5}{3}} + 36C_1 t^2 \ln(t) - 27C_1 t^2 \ln(y^2 + z^2) + 2t^{\frac{2}{3}} y^2 + 2t^{\frac{2}{3}} z^2 + 36C_2 t^2 \right).$

Table 2. Infinitesimal Vectors of Eq. (21) Using X_{13} .

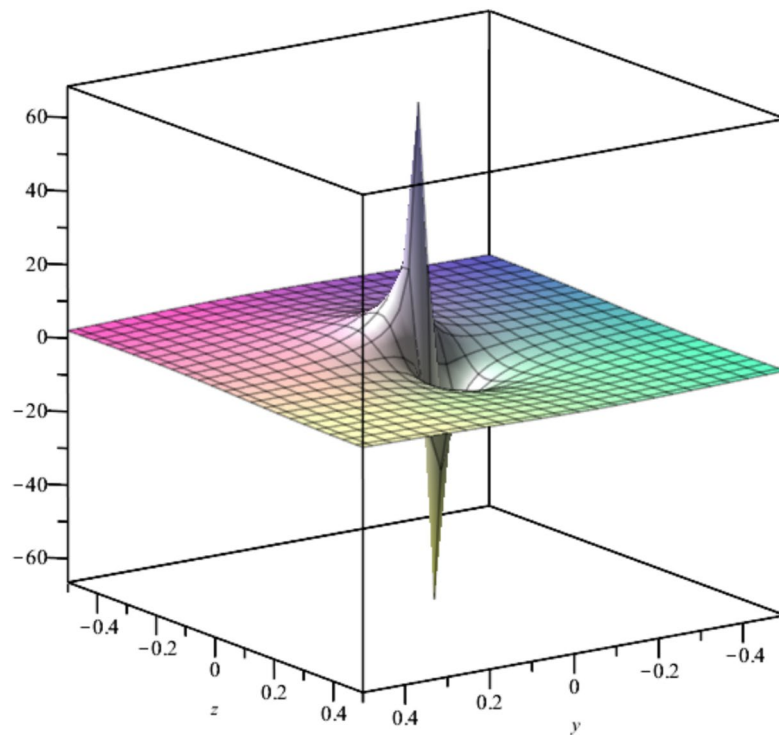


Fig. 8. Illustration of u_8 at $C_0 = 1, C_1 = 1, C_2 = -1, x = 1, t = 1$.

$$u_{14} = \frac{4}{t^{\frac{7}{3}}(4t^2 - 4tz + y^2 + z^2)} \left(t^{\frac{7}{3}} \left(-\frac{2z^2}{3} + z \left(\frac{C_2}{4} - \frac{x}{3} \right) - \frac{2y}{9} \left(y - \frac{9}{8}C_1 - \frac{C_0}{64} \right) \right) \right. \\ \left. + t^{\frac{4}{3}} \left(\frac{xy^2 + xz^2}{12} - \frac{zy^2}{36} + \frac{z^3}{12} \right) + t^{\frac{10}{3}} \left(\frac{x}{3} + \frac{5z}{3} - \frac{C_2}{2} \right) + \frac{C_1}{4} t^{\frac{5}{3}} (y^2 + z^2) \right. \\ \left. + C_1 t^{\frac{11}{3}} - \frac{4}{3} t^{\frac{13}{3}} + C_1 z t^{\frac{8}{3}} + t^{\frac{1}{3}} \left(\frac{y^2 z^2 + y^4}{36} \right) + C_2 y t^3 - C_2 y t^2 z + \frac{C_2 y t}{4} (y^3 + y z^2) \right) \quad (29)$$

$$u_{15} = C_1 t^{\frac{-2}{3}} \ln(4t^2 - 4tz + y^2 + z^2) - \frac{4C_1}{3} t^{\frac{-2}{3}} \ln(t) + C_2 t^{\frac{-2}{3}} + \frac{x}{3t} + \frac{z}{9t} + \frac{y^2 + z^2}{18t^2} - \frac{10}{9}. \quad (30)$$

$$u_{16} = C_2 t^{\frac{-2}{3}} + C_1 y t^{\frac{-4}{3}} + \frac{x}{3t} - \frac{z}{9t} + \frac{z^2}{9t^2} - \frac{8}{9}. \quad (31)$$

Reduction using dual linear combinations of the vectors

Linear combinations of two vectors are used to create more solutions. The optimal combinations are $X_6 + X_{10}, X_7 + X_{10}, X_{10} + X_{12}, X_7 + X_{16}, X_9 + X_{16}, X_{13} + X_{16}$ and $X_{13} + X_{18}$. The reductions and solutions are discussed below.

Case 1: using $X_6 + X_{10}$

The combined vectors result in the following invariant variables:

$$p = t, q = -\frac{z + z^2 + y^2}{2}, r = x + \frac{t}{2} \arctan\left(\frac{2y}{-2z - 1}\right), w(p, q, r) = u(x, y, z, t) + \frac{1}{2} \arctan\left(\frac{2y}{-2z - 1}\right). \quad (32)$$

Equation (1) is now transformed to:

$$(32q - 4) w_{rrrr} + ((32q - 4)w - 4p^2 + 32q - 4) w_{rr} - (64q - 8) \left(\left(q - \frac{1}{8} \right) (w_{qq}) - \frac{1}{2} w_r^2 + w_q - \frac{1}{2} w_{pr} \right) = 0. \quad (33)$$

Now, Eq. (33) is transformed to:

$$-8ov_{oo} + v_{oo} - 8v_o = 0, \quad (34)$$

Where, $o = q, s = p, v(s, o) = w(p, q, r) - \frac{r}{p}$.

Finally, Eq. (34) has the following exact solution:

$$v(s, o) = F_1(s) + \ln\left(o - \frac{1}{8}\right) F_2(o). \quad (35)$$

The final exact solution of Eq. (1) can be formulated as:

$$u_{17} = \frac{x}{t} + F_1(t) - 3\ln(2) F_2(t) + F_2(t) \ln(-4y^2 - 4z^2 - 4z - 1). \quad (36)$$

Where, $F_1(t)$ and $F_2(t)$ are arbitrary functions in their argument.

The solution described by Eq. (36) is depicted in Fig. 9.

Case 2: using $X_7 + X_{10}$

The following solution is obtained.

$$u_{18} = \left(\left(\frac{3}{4}C_1 t^{-\frac{2}{3}} + \frac{1}{36t^2}\right)(1 + 2z - 2y + 2z^2 + 2yy^2) + \frac{1}{3t}(1 + x) + \frac{3}{4}C_1 \ln(2)t^{-\frac{2}{3}} + C_1 t^{-\frac{2}{3}} \ln(t) + 36C_2 t^2 - 1\right). \quad (37)$$

Case 3: using $X_{10} + X_{12}$

The following solutions are obtained.

$$u_{19} = \frac{t^2}{4} - \frac{z}{2} + C_1 \ln\left(4y^2 + (t^2 - 2z)^2\right) + C_2. \quad (38)$$

$$u_{20} = C_1 - 2C_2 \ln(2) - \frac{t}{4} + C_2 \ln\left(t^2 + t(2 + 4z) + 4y^2 + 4z^2 + 4z + 1\right). \quad (39)$$

The solution, u_{19} , is illustrated in Fig. 10.

Case 4: using $X_7 + X_{16}$

The following solution has been created.

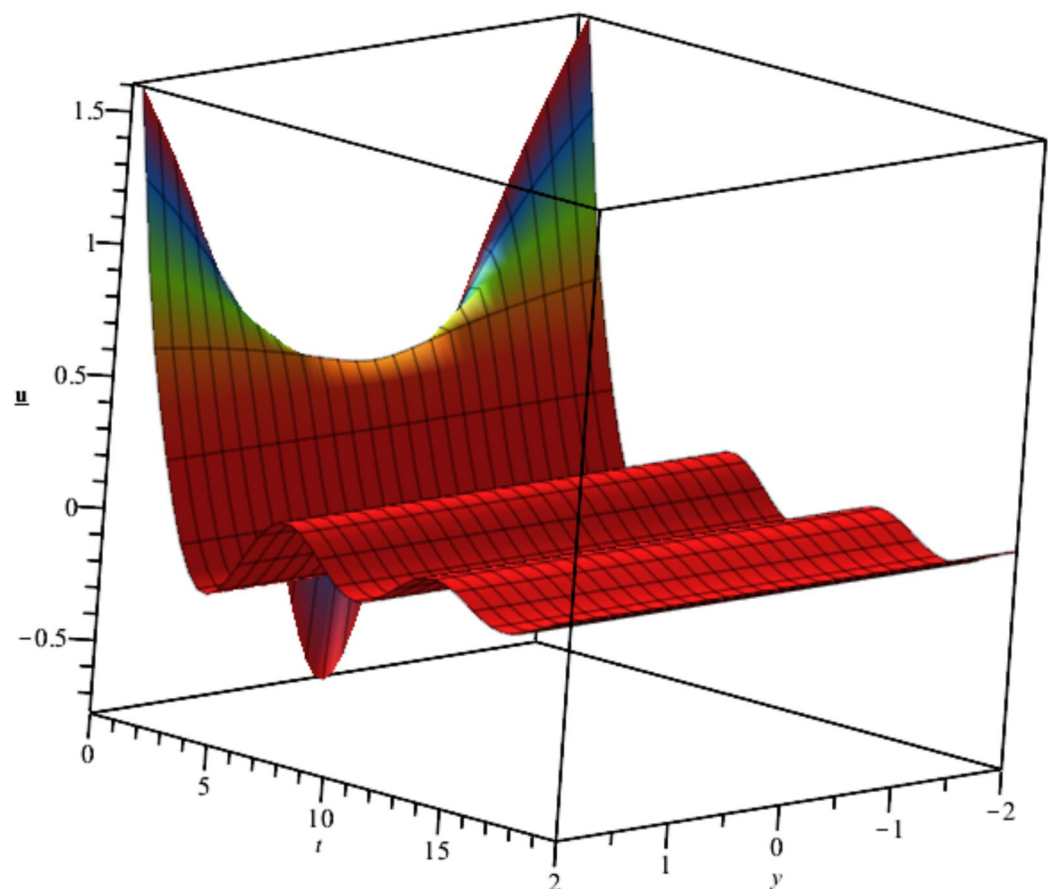


Fig. 9. Illustration of u_{17} at $z = 0, x = 0, F_1(t) = \frac{\sin(t)}{t}, F_2(t) = e^{-t^2}$.

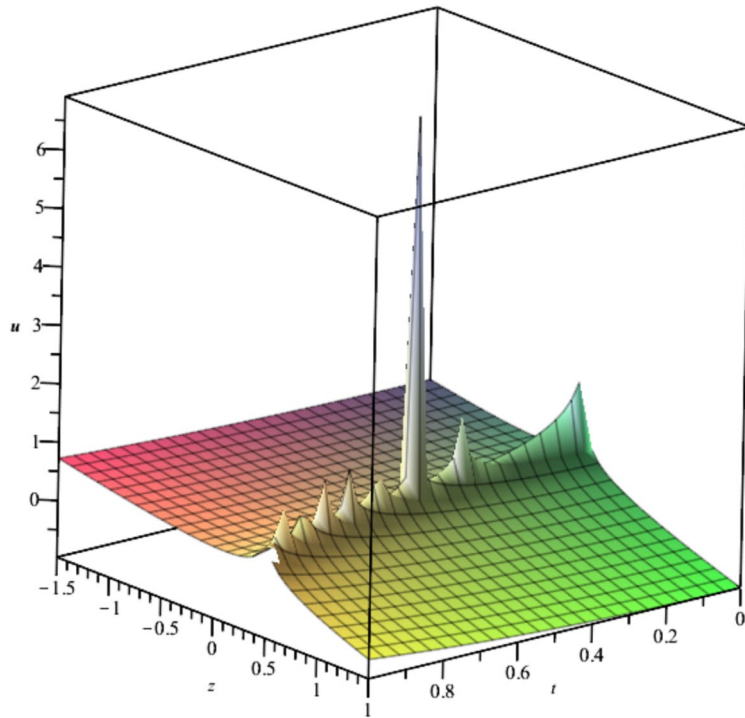


Fig. 10. Illustration of u_{19} at $y = 0, x = 0, C_1 = 0, C_2 = -1$.

$$u_{21} = \frac{864}{(3t+2)^{\frac{7}{3}}(288t^2+t(288-288z)+72y^2+72(z^2-1))} \left(-4t^4+t^3 \left(x+5z-\frac{26}{3}-\frac{3}{2}C_2 \right) \right. \\ + t^2 \left(-\frac{2}{3}y^2+y \left(\frac{C_0}{96}+\frac{3}{4}C_1 \right) + x \left(\frac{5}{3}-z \right) + C_2 \left(\frac{3}{4}z-\frac{11}{4} \right) - 2z^2-7+\frac{25}{3}z \right) \\ + t \left(y^2 \left(\frac{x}{4}-\frac{z}{12}-\frac{5}{6} \right) + y \left(C_1+\frac{C_0}{72} \right) + x \left(\frac{11}{12}+\frac{z^2}{4}-\frac{7z}{6} \right) + C_2 \left(z-\frac{5}{3} \right) + 0.25(z-1) \left(z^2-\frac{25}{3}z+10 \right) \right) \\ + \frac{y^4}{12} + y^2 \left(\frac{z^2}{12}+\frac{x}{6}-\frac{1}{4} \right) + y \left(\frac{C_0}{216}+\frac{C_1}{3} \right) + \frac{1}{6}(z-1)(2+2C_2-3z+z^2+x(z-1)) \\ \left. + (3t+2)^{\frac{1}{3}} + \left(t+\frac{2}{3} \right) \left(3^{\frac{2}{3}}C_2(3t+2)^{\frac{2}{3}}+3^{\frac{4}{3}}C_1y \right) \left(t^2+t(1-z)+\frac{y^2+(z-1)^2}{4} \right) \right). \quad (40)$$

This solution is depicted in Fig. 11 at $C_0 = 0, C_1 = C_2 = 1, x = 0, t = 0$.

Case 5: using $X_{13} + X_{16}$

Employing the same reduction procedures, the following solution is created.

$$u_{21} = \frac{1}{t^{\frac{7}{3}} \left(y^2 + \left(z + \frac{1}{2} \right)^2 \right)} \left(t^{\frac{7}{3}} \left(-\frac{2}{3}y^2 + y \left(C_1 - \frac{C_0}{2} \right) - \frac{2}{3} \left(z + \frac{1}{2} \right) \left(z - \frac{3}{2}C_2 + \frac{1}{2} \right) \right) \right. \\ \left. + \left(y^2 + \left(z + \frac{1}{2} \right)^2 \right) \left(C_1ty + \frac{1}{9}y^2t^{\frac{1}{3}} + \frac{x}{3}t^{\frac{4}{3}} + C_2t^{\frac{5}{3}} \right) \right). \quad (41)$$

This solution is illustrated in Fig. 12 at $t = 1, x = 1, C_0 = 0, C_1 = C_2 = 1$.

Case 6: using $X_{13} + X_{18}$

Another exact solution is formulated after the similarity transformation using the combined vectors, $X_{13} + X_{18}$.

$$u_{22} = \frac{27}{t^{\frac{7}{3}}(72t^2-144tz+72y^2+72z^2)} \left(\left(-\frac{13}{12}z^2+z \left(C_2-\frac{2x}{3} \right) - \frac{23y}{36} \left(y-\frac{36}{23}C_1-\frac{C_0}{46} \right) \right) t^{\frac{7}{3}} \right. \\ + t^{\frac{4}{3}} \left(\frac{1}{3}xy^2+\frac{1}{3}xz^2-\frac{1}{18}y^2z+\frac{1}{6}z^3 \right) + t^{\frac{10}{3}} \left(\frac{x}{3}+\frac{5z}{3}-C_2 \right) + t^{\frac{5}{3}}(y^2+z^2) \\ \left. + C_1t^{\frac{11}{3}}-\frac{3}{4}t^{\frac{13}{3}}-2C_1zt^{\frac{8}{3}}+t^{\frac{1}{3}} \left(\frac{1}{9}y^4+\frac{1}{9}y^2z^2+C_2yt^3-2C_2yt^2z+C_2ty^3+C_2tyz^2 \right) \right). \quad (42)$$

Now, this solution is depicted in Fig. 13.

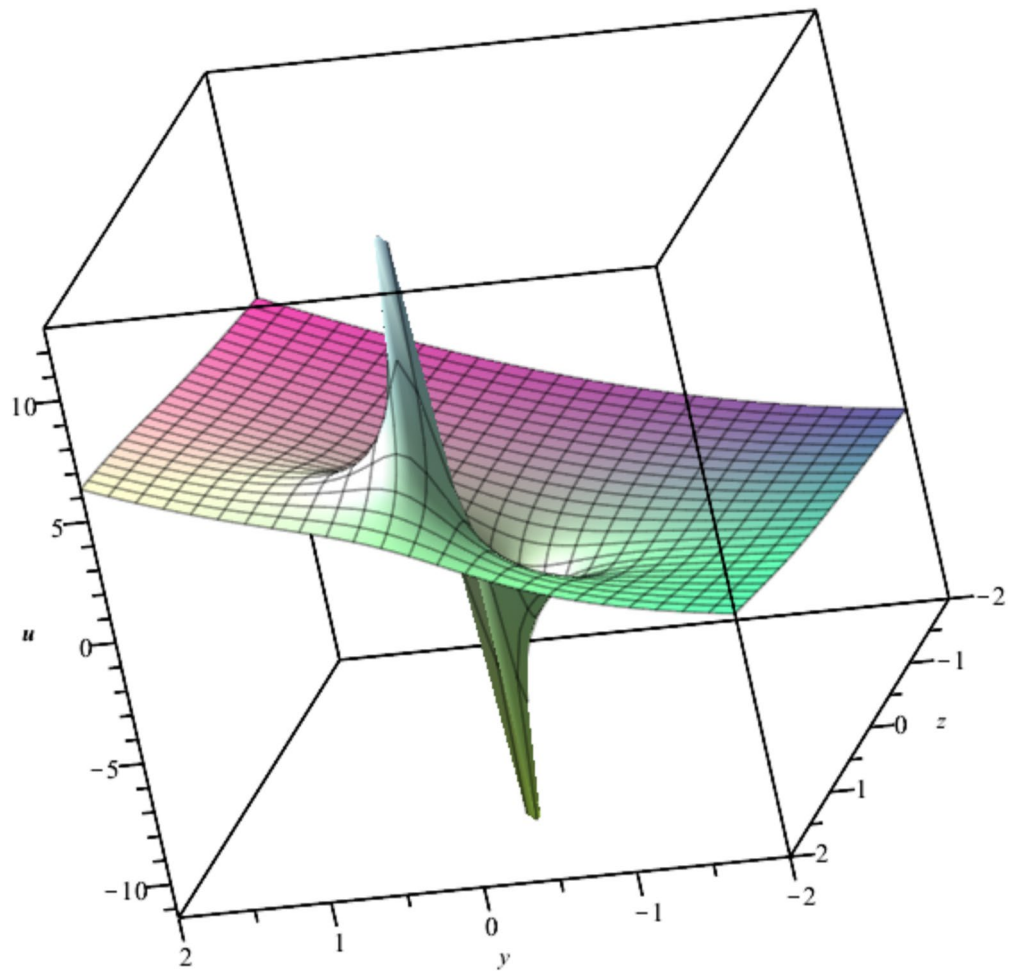


Fig. 11. Illustration of u_{20} at $t = 0, x = 0, C_0 = 0, C_1 = C_2 = 1$.

Reduction using triple linear combinations of vectors

Linear combinations of three vectors are used to create more solutions. The optimal combinations are $X_6 + X_7 + X_{10}, X_6 + X_7 + X_{12}, X_6 + X_{10} + X_{12}, X_7 + X_{10} + X_{12}, X_9 + X_{13} + X_{18}, X_{13} + X_{16} + X_{18}$. The reductions and solutions are described hereafter.

Case 1: using $X_6 + X_7 + X_{10}$

This linear combination leads to the following exact solution.

$$u_{23} = F_2(t) \ln \left(-\frac{3}{2}z^2 - \frac{3}{2}y^2 - z + y - \frac{1}{3} \right) + F_1(t) - \frac{1}{3} \arctan \left(\frac{3y-1}{-3z-1} \right). \quad (43)$$

The solution is depicted in Fig. 14 considering $F_1(t) = \text{sech}^2(t), F_2(t) = e^{-t^2}$ at $y = 0$.

Case 2: using $X_6 + X_7 + X_{12}$

This linear combination leads to the following exact solution.

$$u_{24} = F_2(t) \ln \left(-\frac{1}{6}t^2 - \frac{3}{2}z^2 - zt - \frac{3}{2}y^2 + y - \frac{1}{6} \right) + F_1(t) - \frac{1}{3} \arctan \left(\frac{3y-1}{-3z-t} \right). \quad (44)$$

The solution is depicted in Fig. 15 considering $F_1(t) = \text{sech}^2(t), F_2(t) = \frac{\sin(t)}{t}$ at $z = 0$.

Case 3: using $X_6 + X_{10} + X_{12}$

This linear combination leads to the following exact solution.

$$u_{25} = F_2(t) \ln \left(-\frac{1}{18}t^2 - \frac{1}{2}z^2 - \frac{1}{3}zt - \frac{1}{2}y^2 - \frac{1}{3}z - \frac{1}{9}t - \frac{1}{18} \right) + F_1(t) - \frac{1}{3} \arctan \left(\frac{3y}{-3z-t-1} \right). \quad (45)$$

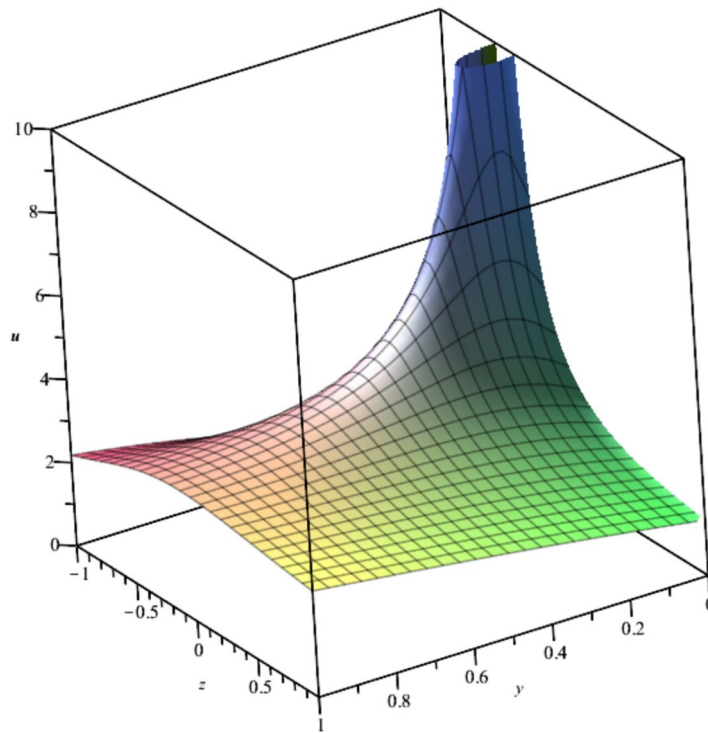


Fig. 12. Illustration of u_{21} at $t = 1, x = 1, C_0 = 0, C_1 = C_2 = 1$.

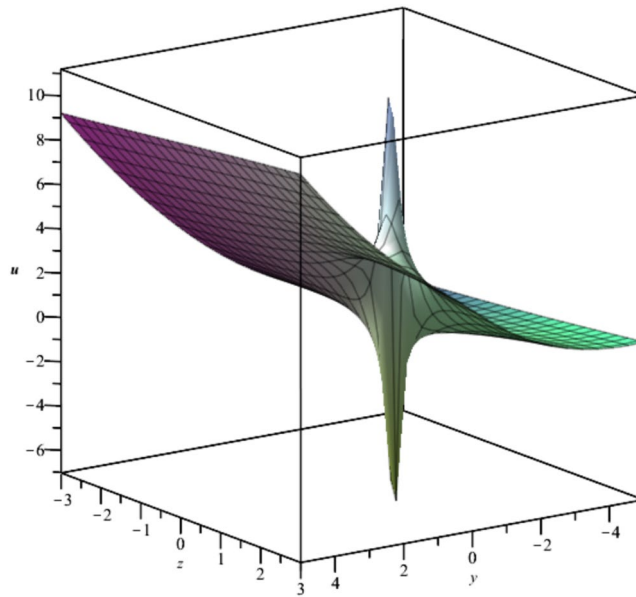


Fig. 13. Illustration of u_{22} at $t = 1, x = 5, C_0 = 0, C_1 = C_2 = 1$.

Case 4: using $X_7 + X_{10} + X_{12}$

Once again, this linear combination leads to the following exact solution.

$$u_{26} = C_1 + C_2 \ln \left(-\frac{1}{6}t^2 - \frac{1}{3}t - \frac{3}{2}z^2 - zt - \frac{3}{2}y^2 - z + y - \frac{1}{3} \right). \quad (46)$$

Case 5: using $X_9 + X_8 + X_{13}$

The following solution is obtained.

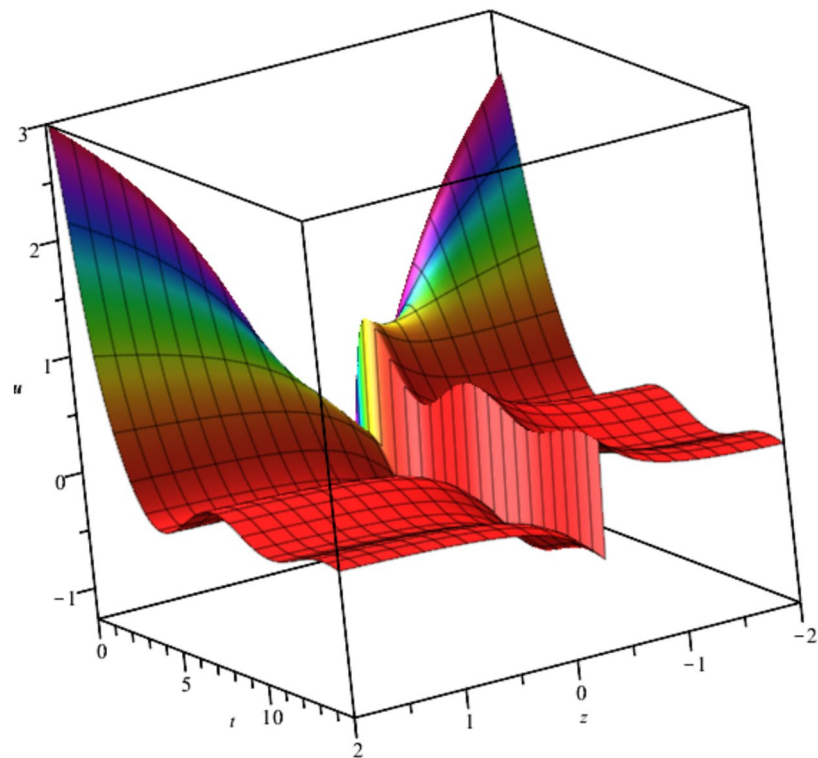


Fig. 14. Illustration of u_{23} at $F_1(t) = \text{sech}^2(t)$, $F_2(t) = e^{-t^2}$ and $y = 0$.

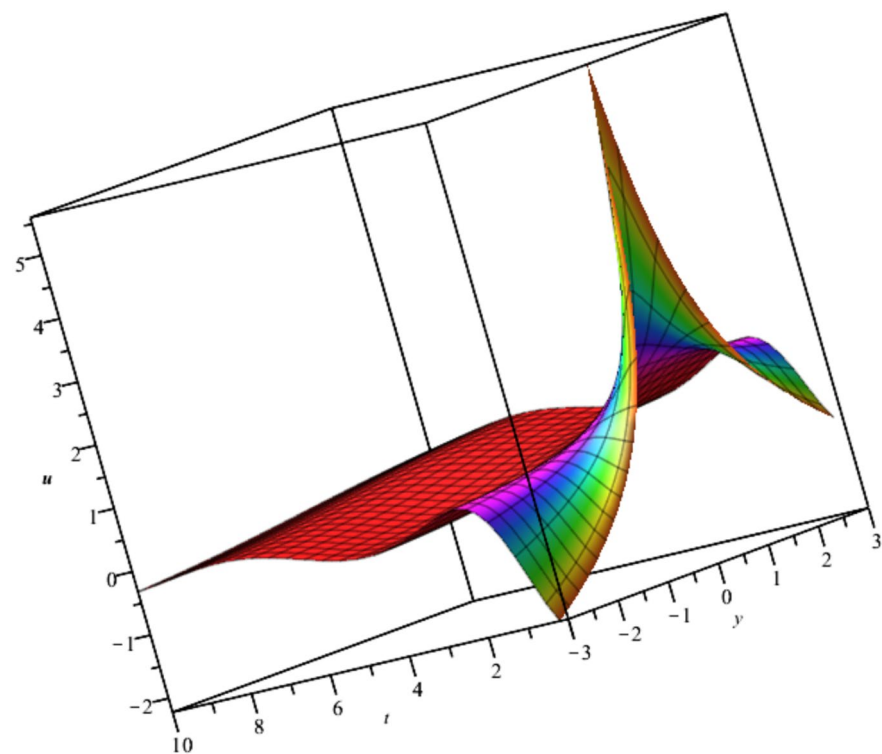


Fig. 15. Illustration of u_{24} at $F_1(t) = \text{sech}^2(t)$, $F_2(t) = \frac{\sin(t)}{t}$ and $z = 0$.

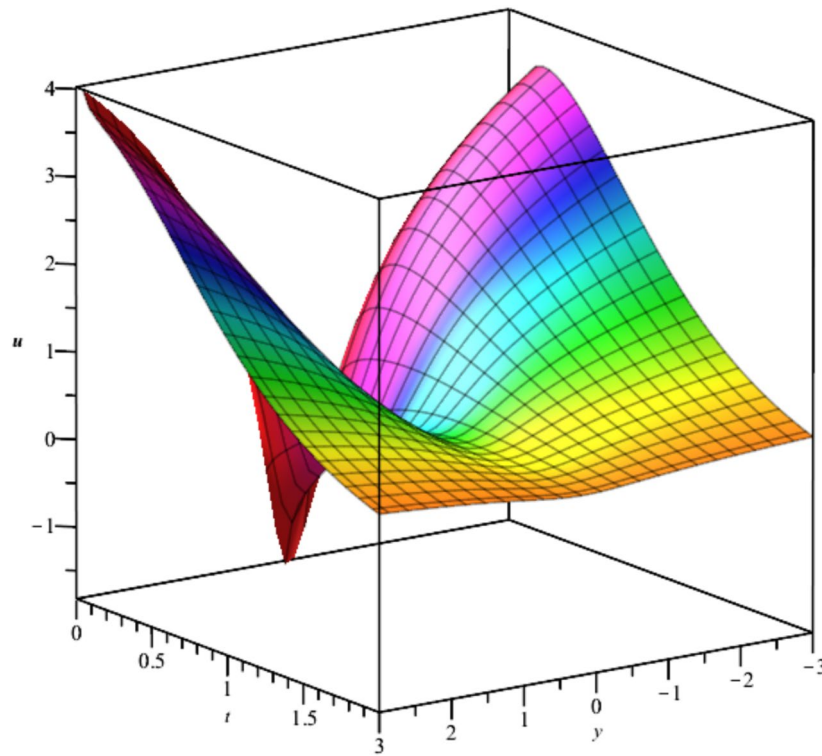


Fig. 16. Illustration of u_{30} at $F_1(t) = \text{sech}^2(t)$, $F_2(t) = \text{sech}(t)$ and $x = 0, z = 0$.

$$u_{27} = \frac{1}{6(3t+1)^2} \left(6 \left(3^{\frac{2}{3}} \right) C_1 (3t+1)^{\frac{4}{3}} \ln(4t^2 + t(4-4z) + y^2 + z^2 - 2z + 1) \right. \\ \left. + 8 \left(3^{\frac{2}{3}} \right) (3t+1)^{\frac{4}{3}} \left(C_1 \ln(3) - C_1 \ln(3t+1) + \frac{3}{4} C_2 \right) - 42t^2 + t(18x + 6z - 42) + 3y^2 + 3z^2 + 6x - 9 \right). \quad (47)$$

$$u_{28} = \frac{3}{(3t+1)^{\frac{7}{3}}} \left((3t+1)^{\frac{1}{3}} \left(-\frac{5}{3}t^2 + t \left(x - \frac{z}{3} - \frac{5}{3} \right) + \frac{z^2}{3} + \frac{x-z+1}{3} \right) + \left(t + \frac{1}{3} \right) \left(C_2(3)^{\frac{2}{3}}(3t+1)^{\frac{2}{3}} + 3^{\frac{4}{3}} C_1 y \right) \right). \quad (48)$$

Case 6: $X_{13} + X_{16} + X_{18}$

This last triple combination leads to the following result.

$$29 = \frac{1}{162t^2} \left(162C_1 t^{\frac{4}{3}} \ln(4t^2 + t(-4-12z) + 9y^2 + 9z^2 + 6z + 1) \right. \\ \left. + t^{\frac{4}{3}} (-324 \ln(3) C_1 - 216 C_1 \ln(t) + 162 C_2) - 128t^2 + t(54x + 6z + 8) + 9y^2 + 9z^2 + 6z + 1 \right). \quad (49)$$

Reduction using quadruple linear combination vectors

A linear combination of four vectors is used to create more solutions. The optimal set of combinations consists of only one combination, $X_{12} + X_{13} + X_{16} + X_{18}$. The solution resulting from using this combination is formulated as:

$$u_{30} = F_2(t) \ln(-t^2 - t(2+8z) - 16y^2 - 16z^2 + 8y - 8z - 2) \\ - 3 \ln(2) F_2(t) + F_1(t) + \frac{1}{32t} \arctan\left(\frac{4y-1}{t+4z+1}\right) + \frac{x}{t} - \frac{z}{8t} - \frac{1}{32t} - \frac{1}{32}. \quad (50)$$

This solution is depicted hereafter in Fig. 16.

Discussion of the results

Bubble creation in liquids is a widespread phenomenon with extensive influence on natural and industrial systems. It facilitates mixing, heat, and mass transport and is therefore essential in processes like chemical reactions, wastewater treatment, and fermentation. In nature, bubbling occurs as submarine volcanism and as part of aquatic life activity. Its dynamics also enable sophisticated applications like ultrasound imaging and drug targeting. Phenomena of gas bubbling need to be mastered to enhance efficiency, safety, and innovation in a multitude of scientific and engineering processes. The optimal system emphasizes obtaining nonrepeated exact solutions^{67,68}. The obtained illustrations, Figs. 1, 2, 3, 4, 5, 6, 7, 8, 9, 10, 11, 12, 13, 14, 15 and 16, introduce

many scenarios of bubble formation in fluids. Figure 1 illustrates gas bubbling through a liquid, with increasing wave-like tendencies in velocity over time and space due to rising gas bubbles that agitate the surrounding liquid. These are typical situations in chemical reactors, bubble columns, and bioreactors, where gas–liquid interaction is a significant factor. Such knowledge can optimize mixing, mass transfer, and reaction rates in industrial processes. Figure 2 presents a pressure or velocity wave propagating in a fluid medium and peaking abruptly. In such cases, a gas bubble rising in a fluid generates oscillatory pressure fields through displacement and buoyant forces. Applications include chemical reactors, underwater acoustics, and medical diagnostics involving microbubbles. Figures 3, 5, 6 and 7 depict several high-frequency oscillating waves with clear peaks and troughs, which are characteristic of complex wave interactions. In gas bubbling in liquids, for instance, such graphs may model turbulence or stochastic waveforms resulting from large numbers of bubbles interacting in a confined area. Sonar and medical ultrasound devices are common applications. Figure 4 displays a single wave representing pressure or velocity distribution caused by the expansion and distortion of a single gas bubble in a viscous liquid. Such waveforms are used to model the initial burst or implosion of bubbles and play a critical role in heat and mass transfer. Fluidized beds, microfluidic devices, and safety analysis in pressurized gas–liquid systems are just a few relevant application areas. Figures 8, 11, and 13 show waves that are likely singularities or steep gradients in fluid behavior, possibly mimicking the pressure or velocity fields around a gas bubble in a fluid. Such dynamics are significant in chemical reactors, underwater acoustics, and biomedical ultrasound. Figure 9 illustrates wave decay with energy loss over time. Applications range from improving aeration in wastewater treatment to optimizing gas delivery in biomedical therapies. Figure 10 shows a localized spike, as observed in gas bubble collapse or microbubble cavitation within a fluid. The transient spike in amplitude suggests concentrated energy over a short timescale, relevant in high-pressure or ultrasonic systems. This is crucial in applications such as medical ultrasound therapy, inkjet printing, and fuel injection systems, where precise bubble dynamics determine performance. In Fig. 11, peaks and steep slopes indicate regions of high intensity—for example, where bubbles rise and create local disturbances. Such wave-like structures can be used to study gas–liquid interactions, mixing efficiency, and bubble plume dynamics. Applications include chemical reactors, wastewater treatment, and bubble column reactor design. Figure 14 reveals oscillations or perturbations at the gas–liquid interface during gas bubbling. The sharp vertical ridges and oscillating surface represent nonlinear wave dynamics or shock-like structures, typically resulting from abrupt gas injection into a viscous fluid. Applications include design optimization of gas sparging in bioreactors and efficiency improvements in fluidized beds and chemical mixing systems. Figures 15 and 16 present dynamic wave profiles, likely modeling fluid surface deformation over time due to gas bubbles rising through a liquid. The steep peaks and troughs indicate local, nonlinear disturbances such as bubble bursts or high-speed jets. Applications include the design of optimized bubble columns, aeration systems, and enhancement of gas–liquid reaction efficiency.

Conclusion

The results obtained by the optimal Lie infinitesimals are divided into four main categories. The reductions and solutions are obtained using single, double, triple, and quadruple linear combinations of the vectors. The resulting closed-form solutions were verified symbolically using the MAPLE package to satisfy the NLWE. These solutions are numerous and diverse in form. Some are expressed as single and multiple solitons, while others appear as singular solitons, or as periodic, logarithmic, exponential, and polynomial waves. Moreover, some solutions are formulated in terms of arbitrary functions, which can be appropriately selected to represent various physical cases. These solutions are particularly important for understanding the behavior of bubbles in gaseous media under different conditions. The chaotic nature of the gaseous medium is the primary reason for the emergence of such varied solutions. The optimal system used is crucial for generating new exact solutions. Higher-order linear combinations lead to more complex solutions of the nonlinear wave equations. However, the number of optimal system members decreases as the order of the linear combination increases, that is, quadruple-vector combinations are fewer than triple, double, or single ones.

Data availability

All data generated or analysed during this study are included in this published article.

Received: 1 May 2025; Accepted: 27 June 2025

Published online: 09 August 2025

References

1. Lauterborn, W. *Cavitation and inhomogeneities* vol. 4, Springer Science & Business Media, Göttingen, Fed. Rep. of Germany, July 9–11, 1979, (2012).
2. Haas, T., Schubert, C., Eickhoff, M. & Pfeifer, H. A review of bubble dynamics in liquid metals. *Metals* **11**, 664 (2021).
3. Davydov, M., Chernov, A. & Pi'nik, A. Dynamics of a gas bubble during fluid decompression at a constant rate. *J. Phys. Conf. Ser.* **1675**, 12030 (2020).
4. Mohammed, W. W., Al-Askar, F. M., Cesarano, C. & El-Morshedy, M. Solitary wave solution of a generalized fractional–stochastic nonlinear wave equation for a liquid with gas bubbles. *Mathematics* **11**(7), 1692 (2023).
5. Shen, G. et al. Abundant soliton wave solutions and the linear superposition principle for generalized (3+1)-d nonlinear wave equation in liquid with gas bubbles by bilinear analysis. *Res. Phys.* **32**, 105066 (2022).
6. Zhao, Y.-H., Mathanaranjan, T., Rezazadeh, H., Akinyemi, L. & Inc, M. New solitary wave solutions and stability analysis for the generalized (3+1)-dimensional nonlinear wave equation in liquid with gas bubbles. *Res. Phys.* **43**, 106083 (2022).
7. Adem, A. R., Podile, T. J. & Muatjetjeja, B. A generalized (3+1)-dimensional nonlinear wave equation in liquid with gas bubbles: Symmetry reductions; exact solutions; conservation laws. *Int. J. Appl. Comput. Math.* **9**(5), 82 (2023).
8. Guo, Y.-R. & Chen, A.-H. Hybrid exact solutions of the (3+1)-dimensional variable-coefficient nonlinear wave equation in liquid with gas bubbles. *Res. Phys.* **23**, 103926 (2021).

9. Liu, W. & Zhang, Y. Resonant multiple wave solutions, complexiton solutions and rogue waves of a generalized (3+1)-dimensional nonlinear wave in liquid with gas bubbles. *Waves Random Complex Media* **30**(3), 470–480 (2020).
10. Zayed, E. M. & Abdelaziz, M. A. Exact solutions for the nonlinear schrödinger equation with variable coefficients using the generalized extended tanh-function, the sine-cosine and the exp-function methods. *Appl. Math. Comput.* **218**(5), 2259–2268 (2011).
11. Betchewe, G., Thomas, B. B., Victor, K. K. & Crepin, K. T. Explicit series solutions to nonlinear evolution equations: The sine-cosine method. *Appl. Math. Comput.* **215**(12), 4239–4247 (2010).
12. Yaghobi Moghaddam, M., Asgari, A. & Yazdani, H. Exact travelling wave solutions for the generalized nonlinear schrödinger (gnls) equation with a source by extended tanh-coth, sine-cosine and exp-function methods. *Appl. Math. Comput.* **210**(2), 422–435 (2009).
13. Taşcan, F. & Bekir, A. Analytic solutions of the (2+1)-dimensional nonlinear evolution equations using the sine-cosine method. *Appl. Math. Comput.* **215**(8), 3134–3139 (2009).
14. Wazwaz, A.-M. The tanh-coth and the sine-cosine methods for kinks, solitons, and periodic solutions for the pochhammer–chree equations. *Appl. Math. Comput.* **195**(1), 24–33 (2008).
15. Wazzan, L. A modified tanh-coth method for solving the kdv and the kdv–burgers' equations. *Commun. Nonlinear Sci. Numer. Simul.* **14**(2), 443–450 (2009).
16. Wazzan, L. A modified tanh-coth method for solving the general burgers–fisher and the kuramoto–sivashinsky equations. *Commun. Nonlinear Sci. Numer. Simul.* **14**(6), 2642–2652 (2009).
17. Bekir, A. & Cevikel, A. C. Solitary wave solutions of two nonlinear physical models by tanh-coth method. *Commun. Nonlinear Sci. Numer. Simul.* **14**(5), 1804–1809 (2009).
18. Kalegowda, B. & Raghavachar, R. Multi-soliton solutions to the generalized boussinesq equation of tenth order. *Comput. Methods Differ. Equ.* **11**(4), 727–737 (2023).
19. Karam Ali, K., Nuruddeen, R. I. & Yildirim, A. On the new extensions to the benjamin–ono equation. *Comput. Methods Differ. Equ.* **8**(3), 424–445 (2020).
20. Sasaki, H. Inverse scattering problems for the hartree equation whose interaction potential decays rapidly. *J. Differ. Equ.* **252**(2), 2004–2023 (2012).
21. Lassas, M., Mueller, J. L., Siltanen, S. & Stahel, A. The novikov–veselov equation and the inverse scattering method, part i: Analysis. *Phys. D* **241**(16), 1322–1335 (2012).
22. Ai, X. & Gui, G. On the inverse scattering problem and the low regularity solutions for the dullin–gottwald–holm equation. *Nonlinear Anal. Real World Appl.* **11**(2), 888–894 (2010).
23. Wazwaz, A.-M. A study on two extensions of the bogoyavlenskii–schief equation. *Commun. Nonlinear Sci. Numer. Simul.* **17**(4), 1500–1505 (2012).
24. Wazwaz, A.-M. Structures of multiple soliton solutions of the generalized, asymmetric and modified nizhnik–novikov–veselov equations. *Appl. Math. Comput.* **218**(22), 11344–11349 (2012).
25. Ma, W.-X., Zhang, Y., Tang, Y. & Tu, J. Hirota bilinear equations with linear subspaces of solutions. *Appl. Math. Comput.* **218**(13), 7174–7183 (2012).
26. Wazwaz, A.-M. N-soliton solutions for the integrable bidirectional sixth-order sawada–kotera equation. *Appl. Math. Comput.* **216**(8), 2317–2320 (2010).
27. Wang, Y. & Wei, L. New exact solutions to the (2+1)-dimensional konopelchenko–dubrovsky equation. *Commun. Nonlinear Sci. Numer. Simul.* **15**(2), 216–224 (2010).
28. Liu, N. General high-order localized waves and interaction solutions to the new (3+1)-dimensional shallow water wave equation in engineering and physics. *Alex. Eng. J.* **114**, 728–737 (2025).
29. Eslami, M., Fathi vajargah, B. & Mirzazadeh, M. Exact solutions of modified zakharov–kuznetsov equation by the homogeneous balance method. *Ain Shams Eng. J.* **5**(1), 221–225 (2014).
30. Zhou, Y., Yang, F. & Liu, Q. Reduction of the sharma–tasso–olver equation and series solutions. *Commun. Nonlinear Sci. Numer. Simul.* **16**(2), 641–646 (2011).
31. Pang, Q. Study on the behavior of oscillating solitons using the (2+1)-dimensional nonlinear system. *Appl. Math. Comput.* **217**(5), 2015–2023 (2010).
32. Abdel Rady, A. S., Osman, E. S. & Khalfallah, M. On soliton solutions for a generalized hirota–satsuma coupled kdv equation. *Commun. Nonlinear Sci. Numer. Simul.* **15**(2), 264–274 (2010).
33. Khalfallah, M. Exact traveling wave solutions of the boussinesq–burgers equation. *Math. Comput. Model.* **49**(3–4), 666–671 (2009).
34. Zhong, W. P., Belic, M. R., Mihalache, D., Malomed, B. A. & Huang, T. W. Varieties of exact solutions for the (2+1)-dimensional nonlinear schrödinger equation with the trapping potential. *Rom. J. Phys.* **64**, 1399 (2012).
35. Mihalache, D. Multidimensional solitons and vortices in nonlocal nonlinear optical media. *Rom. J. Phys.* **59**, 515 (2007).
36. Khan, K. & Ali Akbar, M. Traveling wave solutions of the (2+1)-dimensional zoomeron equation and the burgers equations via the mse method and the exp-function method. *Ain Shams Eng. J.* **5**(1), 247–256 (2014).
37. Parand, K. & Rad, J. A. Exp-function method for some nonlinear pde's and a nonlinear ode's. *J. Saud Univ.—Sci.* **24**(1), 1–10 (2012).
38. Ebaid, A. An improvement on the exp-function method when balancing the highest order linear and nonlinear terms. *J. Math. Anal. Appl.* **392**(1), 1–5 (2012).
39. Biazar, J. & Ayati, Z. Exp and modified exp function methods for nonlinear drinfeld–sokolov system. *J. King Saud Univ.—Sci.* **24**(4), 315–318 (2012).
40. Bhrawy, A. H., Abdelkawy, M. A. & Biswas, A. Cnoidal and snoidal wave solutions to coupled nonlinear wave equations by the extended jacobi's elliptic function method. *Commun. Nonlinear Sci. Numer. Simul.* **18**(4), 915–925 (2013).
41. Gepreel, K. A. & Shehata, A. R. Rational jacobi elliptic solutions for nonlinear differential–difference lattice equations. *Appl. Math. Lett.* **25**(9), 1173–1178 (2012).
42. Elboree, M. K. The jacobi elliptic function method and its application for two component blp hierarchy equations. *Comput. Math. Appl.* **62**(12), 4402–4414 (2011).
43. Rida, S. Z. & Khalfallah, M. New periodic wave and soliton solutions for a kadomtsev–petviashvili (kp) like equation coupled to a schrödinger equation. *Commun. Nonlinear Sci. Numer. Simul.* **15**(10), 2818–2827 (2010).
44. Deng, X., Cao, J. & Li, X. Travelling wave solutions for the nonlinear dispersion drinfeld–sokolov (d(m,n)) system. *Commun. Nonlinear Sci. Numer. Simul.* **15**(2), 281–290 (2010).
45. Abdel Rady, A. S. & Khalfallah, M. On soliton solutions for boussinesq–burgers equations. *Commun. Nonlinear Sci. Numer. Simul.* **15**(4), 886–894 (2010).
46. Cavlak Aslan, E. & Inc, M. Optical solitons and rogue wave solutions of nlse with variable coefficients and modulation instability analysis. *Comput. Methods Differ. Equ.* **10**(4), 905–913 (2022).
47. Singh, M. Multi soliton solutions, bilinear backlund transformation and lax pair of nonlinear evolution equation in (2+1)-dimension. *Comput. Methods Differ. Equ.* **3**(2), 134–146 (2015).
48. Guo, L., Cheng, Y., Mihalache, D. & He, J. Darboux transformation and higher-order solutions of the sasa–satsuma equation. *Rom. J. Phys.* **64**, 104 (2019).
49. Chen, S., Zhou, Y., Baronio, F. & Mihalache, D. Special types of elastic resonant soliton solutions of the kadomtsev–petviashvili ii equation. *Rom. Rep. Phys.* **70**, 16 (2018).

50. Rashed, A. S. Analysis of $(3+1)$ -dimensional unsteady gas flow using optimal system of lie symmetries. *Math. Comput. Simul.* **156**, 327–346 (2019).
51. Kassem, M. M. & Rashed, A. S. N-solitons and cuspon waves solutions of $(2 + 1)$ -dimensional broer–kaup–kupershmidt equations via hidden symmetries of lie optimal system. *Chin. J. Phys.* **57**, 90–104 (2019).
52. Mabrouk, S. M. & Rashed, A. S. Analysis of $(3 + 1)$ -dimensional boiti – leon – manna – pempinelli equation via lax pair investigation and group transformation method. *Comput. Math. Appl.* **74**(10), 2546–2556 (2017).
53. Rashed, A. S. & Kassem, M. M. Hidden symmetries and exact solutions of integro-differential jaulent–miodek evolution equation. *Appl. Math. Comput.* **247**, 1141–1155 (2014).
54. Rashed, A. S. & Kassem, M. M. Group analysis for natural convection from a vertical plate. *J. Comput. Appl. Math.* **222**(2), 392–403 (2008).
55. Kassem, M. M. & Rashed, A. S. Group solution of a time dependent chemical convective process. *Appl. Math. Comput.* **215**(5), 1671–1684 (2009).
56. Inc, M., Hashemi, M. & Isa Aliyu, A. Exact solutions and conservation laws of the bogoyavlenskii equation. *Acta Phys. Polon.* **133**, 1133–1137 (2018).
57. Inc, M., Aliyu, A. I., Yusuf, A. & Baleanu, D. On the classification of conservation laws and soliton solutions of the long short-wave interaction system. *Mod. Phys. Lett. B* **32**(18), 1850202 (2018).
58. Baleanu, D., Inc, M., Yusuf, A. & Aliyu, A. I. Lie symmetry analysis and conservation laws for the time fractional simplified modified kawahara equation. *Open Phys.* **16**(1), 302–310 (2018).
59. Saleh, R., Kassem, M. & Mabrouk, S. Exact solutions of calgero-bogoyavlenskii-schiff equation using the singular manifold method after lie reductions. *Math. Methods Appl. Sci.* **40**(16), 5851–5862 (2017).
60. Saleh, R. & Rashed, A. S. New exact solutions of $(3 + 1)$ -dimensional generalized kadomtsev-petviashvili equation using a combination of lie symmetry and singular manifold methods. *Math. Methods Appl. Sci.* **43**(4), 2045–2055 (2020).
61. Rashed, A. S., Mabrouk, S. M. & Wazwaz, A.-M. Forward scattering for non-linear wave propagation in $(3 + 1)$ -dimensional jimbo-miwa equation using singular manifold and group transformation methods. *Waves Random Complex Media* **32**, 663–675 (2020).
62. Saleh, R., Rashed, A. S. & Wazwaz, A.-M. Plasma-waves evolution and propagation modeled by sixth order ramani and coupled ramani equations using symmetry methods. *Phys. Scr.* **96**(8), 085213 (2021).
63. Rashed, A. S., Mohamed, M. & Inc, M. Plasma particles dispersion based on bogoyavlenskii-konopelchenko mathematical model. *Comput. Methods Differ. Equ.* **12**(3), 561–570 (2024).
64. Mabrouk, S., Rashed, A. & Saleh, R. Unveiling traveling waves and solitons of dirac integrable system via homogenous balance and singular manifolds methods. *Comput. Methods Differ. Equ.* **13**, 72 (2024).
65. Mabrouk, S., Mahdy, M., Rashed, A. & Saleh, R. Exploring high-frequency waves and soliton solutions of fluid turbulence through relaxation medium modeled by vakhnenko-parkes equation. *Comput. Methods Differ. Equ.* **13**, 646–658 (2024).
66. Rashed, A. S. & Kassem, M. M. Similarity transforming techniques of partial differential equations and its applications: A review. *Delta Univ. Sci. J.* **6**(2), 168–181 (2023).
67. Kumar, S. & Rani, S. Symmetries of optimal system, various closed-form solutions, and propagation of different wave profiles for the boussinesq–burgers system in ocean waves. *Phys. Fluids* **34**(3), 037109 (2022).
68. Kumar, S. & Rani, S. Invariance analysis, optimal system, closed-form solutions and dynamical wave structures of a $(2+1)$ -dimensional dissipative long wave system. *Phys. Scr.* **96**(12), 125202 (2021).

Author contributions

E.M.: Conceptualization, Methodology, Writing-Review & Editing, Funding Acquisition. R.S.: Conceptualization, Methodology, Investigation, Formal Analysis, Writing-Original Draft. S.M.: Conceptualization, Methodology, Investigation, Formal Analysis, Investigation, Formal Analysis, Writing-Review & Editing A.S.: Conceptualization, Methodology, Formal Analysis, Investigation, Formal Analysis, Writing-Original Draft, Writing-Review & Editing.

Funding

This work was supported and funded by the Deanship of Scientific Research at Imam Mohammad Ibn Saud Islamic University (IMSIU) (grant number IMSIU-DDRSP2503).

Declarations

Competing interests

The authors declare no competing interests.

Additional information

Correspondence and requests for materials should be addressed to A.S.R.

Reprints and permissions information is available at www.nature.com/reprints.

Publisher's note Springer Nature remains neutral with regard to jurisdictional claims in published maps and institutional affiliations.

Open Access This article is licensed under a Creative Commons Attribution 4.0 International License, which permits use, sharing, adaptation, distribution and reproduction in any medium or format, as long as you give appropriate credit to the original author(s) and the source, provide a link to the Creative Commons licence, and indicate if changes were made. The images or other third party material in this article are included in the article's Creative Commons licence, unless indicated otherwise in a credit line to the material. If material is not included in the article's Creative Commons licence and your intended use is not permitted by statutory regulation or exceeds the permitted use, you will need to obtain permission directly from the copyright holder. To view a copy of this licence, visit <http://creativecommons.org/licenses/by/4.0/>.

© The Author(s) 2025